# Mapping of Quantitative Trait Loci for Traits linked to Fusarium Head Blight Symptoms Evaluation In Barley RILs

Piotr Ogrodowicz[1], Anetta Kuczyńska[1,*], Krzysztof Mikołajczak[1], Tadeusz Adamski[1], Maria Surma[1], Paweł Krajewski[1], Hanna Ćwiek-Kupczyńska[1], Michał Kempa[1], Michał Rokicki[2], Dorota Jasińska[2]

[1] Institute of Plant Genetics, Academy of Sciences, Strzeszynska Str. 34, 60-479 Poznan, Poland

[2] Poznan Plant Breeding Station, Kasztanowa 5, 63-004 Tulce, Poland

*Corresponding author:

Tel.: (+48 61) 65 50 232; e-mail: akuc@igr.poznan.pl

**Abstract**: Fusarium head blight (FHB) is a devastating disease in small grain cereals worldwide. The disease results in the reduction of grain yield and affects its quality. In addition, mycotoxins accumulated in grain are harmful to both humans and animals. It has been reported that response to pathogen infection may be associated with the morphological and developmental characteristics of the host plant, e.g. the earliness and plant height. Despite the many studies the effective markers for the selection of barley genotypes with increased resistance to FHB have not thus far been developed. Therefore, exploring the genetic relationship between agronomic traits (e.g. heading date or stem height) and disease resistance is of importance to the understanding of plant resistance via "diesease escape" or dwarf stature. The studied plant material consisted of 100 recombinant inbred lines (RIL) of spring barley. Plants were examined in field conditions (three locations) in a completely randomized design with three replications. Barley genotypes were artificially infected with spores of *Fusarium* before heading. Apart from the main phenotypic traits (plant height, spike characteristic, grain yield) the infected kernels were visually scored and the content of deoxynivalenol (DON) mycotoxin was investigated. A set of 70 Quantitative Trait Loci (QTLs) were detected through phenotyping of the mapping population in field condition and genotyping using a barley Ilumina iSelect platform with 9K markers. Six loci were detected for FHB index on chromosomes 2H, 3H, 5H and 7H. The region on the short arm of the 2H chromosome was

detected in the current study, in which many QTLs associated with FHB- and yield-related characters were found. This study confirms that agromorphological traits are tightly related to the FHB and should be taken into consideration when breeding barley plants for FHB resistance.

## Introduction

Fusarium head blight (FHB) or a scabs affects different species of crops around the world. The infection is caused by several fungal pathogens, among others *Fusarium culmorum* (W. G. Sm.) *Sacc* and *Fusarium graminearum* (teleomorph stage: *Gibberella zeae*). The first species of *Fusarium* has been found to dominate in regions with warm and humid conditions, whereas the second has been associated with cool, wet and humid conditions [1]. The visible symptoms of the disease are bleaching of some of the florets in the head before maturity stage. Other symptoms include tan to brown discoloration at the base of the spike and a pink or orange colored mold at the base of the florets under moist conditions. Kernels observed on the infected spikes are shriveled, white, and chalky in appearance. Moreover, *Fusarium* spp. produce trichothecene - deoxynivalenol (DON) [2]. This mycotoxin disrupts normal cell function by inhibiting protein synthesis [3] which can result in reducing grain quality and yield performance. Floret sterility and deformed kernels contribute to significant yield loss [4]. In Europe 15 – 55% of the barley products are contaminated with DON [5].

DON poses a real threat to human and livestock health. This mycotoxin is also known as "vomitoxin" due to its emetic effects after consumption [6]. DON levels present in barley (*Hordeum vulgare* L.) and wheat (*Triticum aestivum* L.) infected with FHB may vary according to the time of infection and environmental factors. It is well known that infection is favored by moist and warm conditions [7, 8]. While the presence of scab can be determined through visual inspection, the presence of DON cannot. The assessment of disease severity is based on the ratio of symptomatic spikelets on each spike and the proportion of infected spikes among the tested

plants [9]. Although this method is widely used in the screening of resistant germplasms, the results are subjective. Hence, different types of chromatography for identification and quantification of mycotoxins in barley are commonly in use [10, 11]. However, due to the time-consuming and costly nature of these methods, commercial immunometric assays, such as enzyme-linked immunosorbent assay (ELISA), are frequently used for the monitoring of mycotoxin content [12, 13].

Disease control is achieved by the deployment of resistant cultivars. However, breeding for FHB resistance has proved difficult due to the complex inheritance of the resistance genes [14] and the strong genotype-by-environment interaction [15].

One of the several crop species most vulnerable to FHB infection is barley (*Hordeum vulgare* L.). This species is a cereal crop of major importance, ranked the fourth grain crop in the world in terms of production volume [16]. Its major uses are both as animal feed and as a component of human nutrition [17, 18]. In addition, barley is perceived to be a model plant in genetic study due to genome colinearity and synteny across rye, barley and wheat [19].

Fusarium poses a real threat for barley plants especially in regions that are prone to have long periods of wet weather during the flowering stage [4]. Host plants are most vulnerable to infection during anthesis due to development of fungal spores on anthers and polen containg nutrients [20]. Numerous morphological traits have been shown to be associated with FHB resistance in barley [21]. Heading date, plant height, and spike characters (linked to spike compactness) are mostly investigated [22, 23]. Days to heading is often negatively correlated with FHB susceptibility and usually results in disease escape [24]. Hence, using the least susceptible varieties with different flowering date may reduce FHB risks. Two categories of resistance to FHB are generally recognized: type I (resistance to initial infection) and type II (resistance to fungal spread within the spike) [25]. Another kind of resistance has been described as a third type and is related to the accumulation of mycotoxins within the grains [26].

Studies designed to determine the number and chromosomal location of loci contributing to FHB resistance and the accumulation of DON are urgently needed for the resistance breeding efforts. Resistance to FHB is a complex trait controlled by multiple genes and affected by environmental factors [27, 28]. QTL have been identified for both qualitative and quantitative disease resistance in wheat and barley [4]. Resistance to FHB and DON level content have been mapped to all seven barley chromosomes [29, 30]. The most common regions related to FHB resistane have been previously reported on chromosomes 2H and 6H in many studies [3, 25, 31]. Other traits including awned/awnless ears [26] and spike compactness [32] have also been studied. Plant height is another parameter frequently investigated, and a negative correlation of this trait with Type I FHB susceptibility has been frequently documented [33].

Molecular markers have become increasingly important for plant genome analysis. Different classes of DNA markers have been developed and implemented over time [34]. A new genotyping platform followed in 2009 that introduced larger numbers of markers based on SNP discovery in Next Generation Sequencing data when the Illumina's oligo pool assay as a marker platform [35] was designed to improve the genotyping process. The 9K iSelect chip contains 7864 SNPs [36] and enables higher efficiency and cost reduction. In the current study this chip was employed due to the favorable tradeoff between genotyping costs and marker density.

This study aimed to map quantitative traits loci linked to agronomic properties in mapping population grown in field conditions and subjected to artificial *Fusarium* infection. Evaluation of diease severity was based on both visual assessment of infection and evaluation of deoxynivalenol content.

## Material and methods

Plant material:

A 100-RIL population of spring barley obtained from the cross between the Polish cultivar Lubuski and a Syrian breeding line (Cam/B1/CI08887//CI05761) was studied in field conditions, together with both parental forms. The plant materials were described in detail in Ogrodowicz et al. [37].

Field experiment:

The experiments were perfomed in experimental areas belonging to Poznan Plant Breeding Company (PPB) in three locations: Nagradowice (NAD –Western Poland, 52°19′14″N, 17°08′54″E), Tulce (TUL - Western Poland, 52°20′35.2″N 17°04′32.8″E), Leszno (LES - Western Poland, 51°50′45″N 16°34′50″E). At each location, the experiments were performed in randomized blocks with three replications. The effects of the *Fusarium* infection were evaluated during the 2016 growing season. The two experimental variants were: V1 – variant 1 – control condition, V2 – variant 2 – inoculation. Control rows were established at a distance of 20.0 m from the plots designated for inoculation. This isolation was necessary to protect the plants against infection during inoculation.

Methodology:

Inoculum was prepared just before the inoculations by liquid cultures of *Fusarium culmorum* (isolate KF846) and 0.0125% of TWEEN®20 (Sigma-Aldrich Chemie GmbH). Conidia concentration was adjusted to $10^5$/1 mL. Inoculation was performed at flowering stage (BBCH scale 61). After inoculation the plants were micro-irrigated for three days to maintain moisture.

Agronomic traits:

At maturity, the number of spikelets (NSS), number of kernels (NGS), length of spike without awns (LS) and grain weight per spike (GWS) were observed on 10 randomly selected plants. In addition, during investigation, heading date (HD), plant height (HD) and stature of plants (Stature)

were recorded. Finally, the plots were harvested and grains from trials were weighed to derive grain yield per plot (GY). In our study, two additional traits were added to the analysis: the numbers of sterile spikelets per spike (Sterility) and spike density (Density). The measured traits with ontology annotation are listed in Table 1.

142 Table 1. List of phenotypic traits with description, abbreviations, measured units and ontology annotation.

| Trait (unit) | Trait description | Abbrev | Annotation |
|---|---|---|---|
| Number of spikelets per spike | Number of spikelets in spike from 10 randomly selected spikes in a pot | NSS | http://purl.obolibrary.org/obo/TO_0000456 |
| Number of grains per spike | Number of grains collected from 10 randomly selected spikes in a pot | NGS | http://purl.obolibrary.org/obo/TO_0002759 |
| Length of spike (cm) | Length of spike from 10 randomly selected spikes in a pot (without awns) | LS | http://purl.obolibrary.org/obo/TO_0000040 |
| Fertile and sterile spikelets number per spike | Fraction of sterile spikelets per spike, calculated as a ratio of number of spikelets per spi (NSS) to number of grains per spike (NGS) | Sterility | http://purl.obolibrary.org/obo/TO_0000436 |
| Spike density/the number of spikelets per unit leng (centimeter) of spike | Trait calculated by dividing the number of spikelets per spike by the length of the spike | Density | http://purl.obolibrary.org/obo/TO_0020001 |
| Grain weight per spike (g) | Average weight of grain per spike, calculated from 10 randomly selected spikes in a pot | GWS | http://purl.obolibrary.org/obo/TO_0000589 |
| Grain yield (g) | Weight of grain harvested per plot | GY | http://purl.obolibrary.org/obo/TO_0000396 |
| 1000-grain weight (g) | Average weight of 1000 grains, calculated as 1000 * average weight of one grain for spikes in a pot | TGW | http://purl.obolibrary.org/obo/TO_0000382 |
| Heading date (number of days) | Number of days from sowing to emergence of inflorescence (spike) from the flag leaf ( BBCH), assessed when spikes emerged on at least 50% of plants | HD | http://purl.obolibrary.org/obo/TO_0000137 |
| Length of main stem (cm) | Average of measurements of length of stem from ground level to the end of spike (witho awns) for 10 randomly selected plans in a pot | LSt | http://purl.obolibrary.org/obo/TO_0000576 |
| Stature | Overall size/ shape of plant | Stature | |
| FHB index | Spike infection in % percentage of spikelets affected within a spike / percentage of infect spikes per plot)*100 | FHBi | http://purl.obolibrary.org/obo/TO_0000662 |
| DON concentration (ppb) | Deoxynivalenol content of the grain | DON | http://purl.obolibrary.org/obo/TO_0000669 |
| Number of damaged kernels | Number of kernels classified as damaged (pinkish or discoloured) per 10 randomly select spikes | FDKn | |
| Weight of damaged kernels (g) | Weight of kernels classified as damaged (pinkish or discoloured) per 10 randomly select spikes | FDKw | |
| Number of healthy kernels | Number of kernels classified as healthy per 10 randomly selected spikes | HLKn | |
| Weight of healthy kernels (g) | Weight of kernels classified as healthy per 10 randomly selected spikes | HLKw | |

144 Disease symptoms evaluation:

145 Disease development was visually scored using the Fusarium Head Blight index (FHBi)
146 (percentage of infected spikelets within a spike / percentage of infected spikes per plot) ×100. After
147 harvest Fusarium-damaged kernels (FDK) were observed - the number (FDKn) and weight
148 (FDKw) of kernels, which were classified as pinkish or discoloured (Fig 1, 2). Those kernels that
149 appeared to be healthy were scored as HLK (healthy looking kernels – division: HLKn and
150 HLKw). FDK and HLK rate was estimated for infected and controlled kernels in one location
151 (NAD).

152 DON content (mg $kg^{-1}$ ppm) from infected grain samples (each experiment with three
153 replications) was assessed using a Ridascreen®DON competitive enzyme immunoassay kit (R-
154 Biopharm AG, Darmstadt, Germany) according to the manufacturer's instructions. Absorbance
155 was measured at 450 nm with a spectrophotometer (Chromate Microplate Reader). The data were
156 evaluated with RIDA®SOFT Win software. Within a single locations (NAD, TUL, LES) samples
157 obtained from plants grown in controlled conditions (exposed to natural infection) were pooled
158 together into one repetition and this pool was assayed as above.

159
160
161
162 Fig 1. Seeds, observed in Lcam plants, with moderate or severe *Fusarium* symptoms. Seeds are thin,
163 with some dark discolouration. This image was captured at 40 x magnification under the Motic BA410-E
164 microscope.
165
166
167 Fig 2. Abundant mycelial growth observed on the grain surface. This image was captured at 40 x
168 magnification under the Motic BA410-E microscope.
169
170
171
172 Genotyping:

173 Genomic DNA was extracted from young leaf tissue as described in Mikołajczak et al. 2016 [38].
174 DNA quantity and concentration were measured with a NanoDrop 2000 (Thermo Scientific™).

175 The DNA samples were diluted to ~ 50 ng/µL and sent to Trait Genetics, Gatersleben, Germany
176 (http://www.traitgenetics.com). The barley iSelect SNP chip contains a total of 7.842 SNPs that
177 comprise 2.832 of the existing barley oligonucleotide pooled assay (BOPA1 and BOPA2) SNPs
178 discovered and mapped previously [39, 40], plus 5.010 new SNPs developed from Next
179 Generation Sequencing data [36, 41]. SNPs which were not polymorphic between the parents,
180 contained more than 10% of missing values, or with minor allele frequency smaller than 15% were
181 removed from the markers set.
182
183 Map construction:
184 Genetic maps were calculated using the JoinMap 4.1 software [42]. All markers were analyzed for
185 their goodness of fit using a chi-square test at significance level $\alpha = 0.05$. A segregation ratio of
186 1:1 was expected. Markers with other segregation ratios were categorized as odd. The markers
187 which were mapped to incorrect regions of the chromosomes were removed from the mapping and
188 the marker order was calculated again. The localization of markers was designated using the
189 maximum likelihood algorithm command. Markers were assigned to linkage groups applying the
190 independence LOD (logarithm of the odds) parameter with LOD threshold values ranging from
191 6.0 to 9.0. The recombination frequency threshold was set at level $\leq 4$. Recombination fractions
192 were converted to map distances in centimorgans (cM) using the Kosambi mapping function. A
193 map was drawn using MapChart 2.2
194
195 Data analysis and QTLs mapping:
196 Observations for RILs were processed by analysis of variance in a mixed model with fixed effects
197 for location, treatment and location × treatment interaction, and with random effects for line and
198 interaction of line with location and interaction of line with location and treatment. The residual
199 maximum likelihood algorithm was used to estimate variance components for random effects and
200 the F-statistic was computed to assess the significance of the fixed effects. Pearson correlation

coefficients between all the analyzed traits were calculated. QTL analysis was performed for the linkage map with the mixed model approach described by Malosetti et al. [43], including optimal genetic correlation structure selection and significance threshold estimation. The threshold forthe−log10(P-value) statistic was computed by the method of Li and Ji [44] to ensure the genome-wide error rate was less than 0.01. Selection of the set of QTL effects in the final model was performed at $P<0.05$; the P-values for the Wald test were computed as the mean from the values obtained by adding and dropping the QTL main and interaction effects in the model. All the above computations were performed in Genstat 16 [45]. RIL lines where the lack of genotypic data did not exceed 20/15% were used to map QTL. QTL identification was performed for all studied traits.

The detected QTLs were labeled using a system described for wheat and *Arabidopsis* [46, 47], with minor modifications. The QTLs names consist of the prefix Q followed by a two- or three-letter descriptor of the phenotype (abbreviation of the trait name), an indicator for the laboratory, the number of the chromosome and a serial number. For traits linked to FDK and HLK the QTL names were extended by adding the letter “w” or “n” for loci found for trait weight of FDK, HLK and number of FDK, HLK, respectively.

QTL effects in individual trials were considered major if the fraction of explained variance exceeded 12.32% (upper quartile of the distribution of explained variance) according to the rules employed by [48] and [49] (with minor modifications).

The barleymap pipeline (http://floresta.eead.csic.es/barleymap) [50] was used to identify potential candidate genes underlying the particularly robust QTL of this study. Markers from seven regions harboring QTLs for studied traits were annotated and the gene search was extended to an interval of ±2cM around markers. Overrepresentation analysis (ORA) of GO terms (among high confidence gene class) was performed using the hypergeometric distribution [51, 52] and applying the Benjamini–Hochberg correction (FDR level of 0.05) [53].

# Results

Phenotypic analysis:

The parents of the LCam population were characterized with 11 agronomical traits under two different conditions (infection and control treatments). Evaluation of disease severity was studied by using measurements of six FHB-related traits in both type of previously mentioned conditions. The distributions of trait values among RILs are visualized in Fig 3.

Fig 3. Violin plots for studied traits measured in the LCam population in control (V1, green color) and infected (V2, red color) conditions in three locations. Black symbols: triangle - Lubuski, dot - CamB.

The parental forms were differentiated in terms of all the studied characters (S1 Table). Lubuski showed higher mean values of traits linked to yield performance (e.g. GWS, GY,). The Syrian genotype showed a lower mean value of HD in all trials and under both types of treatments (heading for CamB was 11 days earlier than for Lubuski).

A substantial GY decline was observed for Lubuski in infection condition (40.1%). In comparison, for CamB a lower relative decline for GY was observed (17.3%). Both mean value for FHBi and traits associated with visual evaluation of *Fusarium* symptoms (FDK) increased in the infection conditions. For the Syrian parent a higher mean value of DON concentration was noted in comparison to that of European parent. For both parental forms low concentrations of mycotoxin were also observed in control conditions.

The mean values of the studied traits for RILs are presented in S2 Table. Relatively high values of variation coefficients were observed in location NAD under infection for traits: NSS, NGS, Density, GWS and TGW. In the LES location very high values of CV were noted for traits FHBi and DON in control conditions.

254 FHBi varied across locations with the mean FHBi ranging from 1.89 to 2.26 under infection
255 treatment and from 0.62 to 0.99 in control condition (S2 Table).The amount of DON, measured in
256 grains from infected plants, varied from a maximum of 39990.00 µg kg−1 (TUL) to 8060.00 µg
257 kg−1 (NAD). Mean DON values of 26 439.47, 25 684.27 and 27 144.47 µg kg−1 for infection
258 treatment in LES, NAD, TUL were observed, respectively. In control conditions relatively high
259 coefficients of variation were noted for DON and FHBi.

260 Analysis of variance indicated significant effects of location and treatment on the RIL
261 population for all traits ($P<0.001$) with several exceptions (Table 2). In all cases, the variance
262 components for all types of interactions were smaller than those for lines. For FHBi a significant
263 line × location interaction was noted. No signicant interaction was observed for line × treatment
264 in this case. An insigificant effect was noticed in terms of the interaction line × location for DON
265 content.

266 Correlations (based on the mean values for lines over locations) between the studied traits
267 and FHBi were statistically significant in two types of treatments but values were generally low
268 (Table 3). FHBi was negatively correlated with NSS, NGS, Sterility, Density, GWS, GY, HD and
269 LSt at least in one type of treatment. Significant positive correlations were recorded between FHBi
270 and Sterility in both control and infected conditions. Correlations between FHBi and *Fusarium*
271 severity parameters (FDKn, FDKw, HLKn, HLKw) were significant under both type of treatments
272 (an exception: HLKw in control condition). Positive, marginal correlations were found between
273 FHBi and traits linked to FDK (FDKw and FDKn). HLKn and HLKw showed moderate
274 correlations with FHBi.

275

276

277 Table 2. ANOVA results and variance components estimated for studied traits

| Trait (abbrev. | P-values for effects of | | | Variance components and std. errors for | | | | | | | |
|---|---|---|---|---|---|---|---|---|---|---|---|
| | location | treatment | location × treatment interacton | lines | s.e. | interaction line x location | s.e. | interaction line x treatment | s.e. | interaction line location × treatm | s.e. |
| NSS | <0.001 | <0.001 | <0.001 | 2.447 | 0.397 | 0.32 | 0.135 | 0.02 | 0.093 | 0 | - |
| NGS | <0.001 | <0.001 | <0.001 | 2.766 | 0.446 | 0.394 | 0.143 | 0.033 | 0.096 | 0 | - |
| LS | <0.001 | <0.001 | <0.001 | 0.2643 | 0.0443 | 0.0634 | 0.0178 | 0 | - | 0.0181 | 0.0194 |
| Sterility | <0.001 | <0.001 | <0.001 | 0.000139 | 0.00005 | 0.000251 | 0.000065 | 0 | - | 0 | - |
| Density | <0.001 | 0.138 | 0.009 | 0.0256 | 0.00448 | 0.0056 | 0.00176 | 0.0022 | 0.00135 | 0 | - |
| GWS | <0.001 | <0.001 | <0.001 | 0.00969 | 0.00167 | 0.00144 | 0.0065 | 0.00065 | 0.00052 | 0 | - |
| GY | <0.001 | <0.001 | 0.006 | 329.9 | 52.8 | 0 | - | 0 | - | 0 | - |
| TGW | <0.001 | <0.001 | <0.001 | 1.9 | 0.87 | 1.22 | 1.03 | 0.97 | 0.88 | 0 | - |
| Stature | 0.927 | 0.15 | 0.31 | 3.05756 | 0.44322 | 0.25067 | 0.02747 | 0 | - | 0.02229 | 0.00496 |
| HD | <0.001 | <0.001 | 0.035 | 9.625 | 1.419 | 1.142 | 0.134 | 0.013 | 0.024 | 0.019 | 0.041 |
| LSt | <0.001 | <0.001 | <0.001 | 9.55 | 2.047 | 5.118 | 1.414 | 0.519 | 0.881 | 11.234 | 1.425 |
| FHBi | <0.001 | <0.001 | 0.02 | 0.0471 | 0.0325 | 0.4351 | 0.0461 | 0.0045 | 0.0037 | 0.0187 | 0.0056 |
| $DON_x$ | <0.001 | | | 21271008 | 3204801 | 0 | - | - | - | | |
| FDKn | - | <0.001 | - | 0.000228 | 0.000082 | - | - | 0.000189 | 0.000084 | - | - |
| FDKw | - | <0.001 | - | 0.0000157 | 0.00000595 | - | - | 0.00001913 | 0.00000611 | - | - |
| HLKn | - | <0.001 | - | 2.568 | 0.494 | - | - | 0.248 | 0.256 | - | - |
| HLKw | - | <0.001 | - | 0.00645 | 0.00231 | - | - | 0.00161 | 0.00244 | - | - |

278 * variance component at least three times greater than its standard error
279 s.e.- standard error
280 $_x$- ANOVA analysis only for infection condition
281
282

Table 3. Correlation coefficients between FHB and studied traits recorded in two types of treatments.

| Trait | Treatment | |
|---|---|---|
| | Infection | Control |
| NSS | -0.46 | -0.32 |
| NGS | -0.52 | -0.35 |
| LS | n.s. | n.s. |
| Sterility | 0.52 | 0.31 |
| Density | -0.43 | -0.27 |
| GWS | -0.44 | -0.35 |
| GY | -0.25 | -0.32 |
| TGW | n.s. | n.s. |
| Stature | -0.26 | n.s. |
| HD | -0.46 | -0.42 |
| LSt | -0.28 | n.s. |
| DON | n.s. | n.s. |
| FDKn | 0.25 | 0.26 |
| FDKw | 0.28 | 0.23 |
| HLKn | -0.46 | -0.42 |
| HLKw | -0.48 | n.s. |

n.s.- not significant

Correlations shown are significant at the P<0.01 level

Linkage map construction:

The constructed genetic map comprised of 1947 SNPs distributed on seven linkage groups. The map length was 1678 cM with an average marker interval of 0.86 cM. The shortest chromosome was 6H, which harbored 250 markers with a genetic length of 141 cM and an average interloci distance of 0.56 cM. The longest chromosome was 2H, and it harbored 368 markers with a genetic length of 291 cM and an average interloci distance of 0.79 cM. The number of markers, marker density and map length for individual chromosomes are listed in Table 4.

Table 4. Map details across each chromosome

| | Chromosome | | | | | | | Total |
|---|---|---|---|---|---|---|---|---|
| | 1H | 2H | 3H | 4H | 5H | 6H | 7H | |
| Number of mapped markers | 156 | 368 | 324 | 329 | 324 | 250 | 196 | 1947 |
| Map lenght (cM) | 232 | 291 | 241 | 215 | 295 | 141 | 263 | 1678 |
| Mean distance between markers (cM) | 1.48 | 0.79 | 0.74 | 0.65 | 0.91 | 0.56 | 1.30 | 0.86 |

## QTL analysis

A total of 70 QTLs for all studied traits were found for the LCam population. The numbers of QTLs were 7, 24, 5, 6, 17, 4, and 7 for chromosomes 1H, 2H, 3H, 4H, 5H, 6H and 7H, respectively. Moreover, 46 QTLs presented main effects and 38 presented QTL × E interaction. The largest number of QTLs was detected for NSS and TGW (eight QTLs were identified for each trait), and the smallest for FDK (two QTLs were detected for FDKn and FDKw). 14 QTLs were classified as major loci and 56 QTLs were decribed as minor loci. Detailed information, including location, peak marker, additive effects and explained phenotypic variance for each QTL and trait is presented in S3 Table.

S3 Table . QTLs identified in the LCam population for the observed traits.

*Spike characteristics*

For the number of spikelets per spike eight QTLs were detected, in chromosomes 1H, 2H, 3H, and 5H. The major QTL (QNSS.IPG-2H_1) on chromosome 2H (SNP marker BK_12) showed the most significant effect for this trait and explained a large proportion of the phenotypic variance (4.79-71.81%). In this case significant QTL × E interaction was noted. A second locus positioned at 98.67 cM on chromosome 5H also showed a highly significant association with NSS (LogP statistics = 16.95). Chromosome 1H was the location of the last major QTL (QNSS.IPG-1H_1) in the vicinity of marker BOPA1_4625-1413. The remaining five NSS QTLs showed minor effects. Out of the eight QTLs detected for NSS, three (QNSS.IPG-1H_2, QNSS.IPG-2H_2 and QNSS.IPG-3H_2) were associated with a significant increase in this trait contributed by Syrian parent alleles.

Five QTLs were found for the number of grains per spike. QNGS.IPG-2H was found in the vicinity of marker BK_12. This locus was positioned at 22 cM on chromosome 2H. The second

major QTL was detected on chromosome 5H in the vicinity of marker BOPA2_12_30929. For this QTL no significant additive effects were recorded in NAD location. The other QTLs (QNGS.IPG-1H_1, QNGS.IPG-1H_2 and QNGS.IPG-5H_2) were classified as minor QTLs. All studied QTLs for NGS were with alleles of European genotype contributing to an increasing of number of grains per spike.

Three QTLs were reported for the length of spike (QLS.IPG-1H, QLS.IPG-2H and QLS.IPG-5H). All detected loci were classiefied as major (≥12.32% PVE) and the effects of these QTLs were stable over environments (treatments). All QTLs were associated wih a significant increase in LS contributed by Lubuski. The main QTL was found n chromosome 2H in the vicinity of marker BK_13. In total, five QTLs were identified for sterility. On chromosome 2H, two major QTLs were detected (QSte.IPG-2H_1 and QSte.IPG-2H_2). The first QTL, QSte.IPG-2H_1, was located in the vicinity of marker SCRI_RS_154030 and showed the highest LogP value of all detected QTLs controlling this trait. The second sterility QTL was located on chromosome 2H 5.6 cM from marker SCRI_RS_230497. One major QTL (QSte.IPG-5H_2) was detected on chromosome 5H. None of the mentioned QTLs had significant additive effects in control condition in LES location and in infection conditions in NAD location. On chromosome 7H, a minor QTL for sterility was identified − QSte. IPG-7H. All QTLs detected for this character were with alleles of Syrian genotype contributing to the increase in sterility with the exception of QSte.IPG-5H_1, where Lubuski alleles determined the increase. Interaction with the environment was found for all but one detected QTLs (an exeption was QSte.IPG-7H).

Six QTLs controlling density were detected on chromosomes 2H and 5H with a PVE ranging from 0.01 to 31.43%. Half of those QTLs displayed significant QTL × E interaction. The main QTL (LogP=15.17) was found on the upper arm of chromosome 2H mapped in marker BK_22. Concurrently, this QTL was the only locus associated with Density, where Lubuski alleles conferred a positive effect in increasing this trait, while the Syrian parent alleles at the other five

QTLs contributed positively to Density. The second major QTL (QDen.IPG-2H_2) was also found on chromosome 2H at position 113.9 cM. On chromosome 2H two other minor QTLs were identified for Density QTL (QDen.IPG-2H_2 and QDen.IPG -2H_4) with a stable effect, mapped in the vicinity of BOPA1_5537-283. QDen.IPG -5H_1 was also found on chromosome 5H at position 93.9 cM. The additive effects of this QTL was signifiant only in two location (NAD and TUL). For Density two minor QTLs were found − QDen.IPG-2H_3 and QDen.IPG-5H_2, for which the smallest LogP values were recorded for Density in this study.

*Grain traits*

Grain weight per spike was mapped to seven loci. The main GWS QTL (QGWS.IPG-2H_1) was found on chromosome 2H in the vicinity of marker BK_22. This locus, with a PVE ranging from 31.74 – 57.92%, was the only GWS QTL where no significant QTL × E interaction was detected. QGWS.IPG-5H was found on chromosome 5H and the nearest marker (BOPA1_4795-782) was 1.37 cM away from the corresponding QTL peak. Two other major QTLs (QGWS.IPG-7H_1 and QGWS.IPG-7H_2) controlling GWS were reported on chromosome 7H. Both of these QTLs had a significant additive effect only in single location. Minor QGWS.IPG-4H_2 was found on chromosome 4H at position 127.40 cM. The European parent contributed to the increase in GWS for all detected QTLs for this trait (exceptions: two QTLs – minor QGWS.IPG -2H_2 and major QGWS.IPG-4H_1 identified on chromosomes 2H and 4H, respectively).

Out of four QTLs found for grain yield, only one was classiefied as major (PVE>12.32%). In additon, no significant additive effects were noticed for any detected loci in infection conditions for NAD location. The main QGY.IPG-2H was located on chromosome 2H and linked to marker BK_22. No QTL × E interaction was found for GWS QTLs detected in the mapping population and in all cases positive alleles were attributed to European parents.

374 Eight QTLs were reported for thousand grain weight. QTGW.IPG-2H_1 and QTGW.IPG-
375 4H_1 were identified on chromosomes 2H and 4H, respectively, but their additive effects were
376 significant only in infection (LES) and control conditions (NAD). On chromosome 4H, TGW QTL
377 was found with a stable and positive effect from the Lubuski genotype. QTGW.IPG-6H_2 locus
378 on chromosome 6H was determined by Syrian parent genotype alleles contributing positively to
379 TGW. In this locus no significant QTL × environment interaction for TGW was also observed.
380 Major QTGW.IPG-7H_1 with stable effects from the CamB allele significantly increasing TGW
381 was identified on chromosome 7H. On the same chromosome was found QTGW.IPG-7H_2, but
382 the additive effects of this QTL were significant only in three treatments. QTGW.IPG-2H_2 and
383 QTGW.IPG-6H_1, detected on chromosome 2H and 6H, respectively, were classiefied as minor
384 QTLs.
385
386 *Heading day and height*
387 Two QTLs (QHD.IPG-2H and QHD.IPG-5H) were reported for heading date. The main QTL was
388 located on chromosome 2H in the vicinity of marker BK_22. The „late" allele (high HD value)
389 was contributed by European parent. In contrast, at the second locus, classified as a minor QTL,
390 the CamB alleles conferred a positive effect by increasing this trait. For both loci, no QTL × E
391 interaction was detected.
392 Seven loci for length of main stem were found in the LCam population. The main locus
393 (QLSt.IPG-2H_1) was detected on chromosome 2H in the vicinity of marker BK_13 at position
394 21 cM. This QTL explained a large portion of the variance for LSt (from 13.88 to 41.68%). The
395 Lubuski alleles contributed to the increase in LSt at this locus. The second major QTL was reported
396 on chromosome 1H with stable and positive effects on the length of the main stem contributed by
397 the European parent genotype. QLSt.IPG-4H_2 and QLSt.IPG-5H were identified on
398 chromosomes 4H and 5H, respectively. These QTLs were classified as major loci, but their
399 additive effects were not significant in some treatments (e.g. control conditions in NAD location).

Three minor LSt loci were found − QLSt.IPG-2H_2, QLSt.IPG-3H and QLSt.IPG-4H_1 detected on chromosomes 2H, 3H and 4H, respectively.

*Fusarium symptoms and DON content*

Six QTLs were reported for the FHB index. The main QTL (QFHBi.IPG-2H_1) was found on chromosome 2H in the vicinity of marker BOPA1_5880-2547 at position 23.10 cM. The CamB alleles positively contributed to the increase in the FHB index at this locus and significant QTL × E interaction was detected for QFHBi.IPG-2H_1. On the same chromosome another FHBi QTL was reported which was located at position 87.70 cM but additive effects of this locus were significant only in one location (TUL). The next major locus (QFHBi.IPG-2H_3) was also detected on chromosome 2H with stable and positive effects of Syrian parent alleles responsible for increasing the FHBi. In contrast, the European parent alleles conferred a positive effect in increasing the FHBi at the locus found on chromosome 5H (QFHBi.IPG-5H). For this QTL no significant additive effects were detected in LES location. Two minor loci − QFHBi.IPG-3H and QFHBi.IPG-7H were reported on chromosome 3H and 7H, respectively.

Four QTLs were found for traits linked to *Fusarium* damaged kernels. These loci were located on chromosomes 5H and 6H. The main QFDKn.IPG-5H was detected in the vicinity of SCRI_RS_165578, where Lubuski genotype significantly increased the FDKn. The second major locus (QFDKw.IPG-5H) was identified at the position 87.80 cM and showed positive effects on this trait contributed by European parent alleles. Two remaining loci found on chromosome 6H (QFDKn.IPG-6H and QFDKw.IPG-6H) were classified as minor QTLs.

Five QTLs were detected for traits associated with healthy looking kernels (HLKw and HLKn). The main QHLKn.IPG-2H_2 was found on the short arm of chromosome 2H (marker BK_13) and showed stable and positive effects of Lubuski genotype alleles which contributed to the increase in HLKn. Two minor QTLs were recorded for HLKn on chromosomes 2H and 5H.

For both loci no significant QTL x E interaction was detected. Two major loci (QHLKw.IPG-2H and Q_HLKw.IPG-7H) were found for the trait HLKw. The Lubuski alleles were responsible for increasing HLKw in both loci but only one QTL (QHLKw.IPG-2H) had stable effects.

Co-localized or pleiotropic QTLs

A total of eight chromosomal regions (named A-G) harboring QTLs for studied traits were assigned. These regions (hotspots), listed in Table 5, were designed based on their proximity to each other (0-5 cM).

Five QTLs were reported in region A located on the top of chromosome 1H, namely associated with SNP BOPA1_4625-1413. Region B identified on the upper arm of chromosome 2H contained to 10 loci. In most cases, QTLs from region B were detected in the vicinity of marker BK_12 (Fig 4). Out of the five QTLs detected in region C assigned on the same chromosome, four were found in the vicinity of marker BOPA2_12_10937. Region D harbored two QTLs found at the same position (127.40 cM) but these loci were linked to different SNP markers. Region E (chromosome 5H) harbored six QTLs – both QDen.IPG-5H_1 and QFHB.IPG-5H were found in this region in the vicinity of marker SCRI_RS_184066 and both QNGS.IPG-5H_1 and QLSt.IPG-5H were detected in the vicinity of marker BOPA2_12_30929. On the same chromosome, the next region was noted (named region F). Out of the four QTLs reported on this region, two were found in the vicinity of marker SCRI_RS_206867. Region F on chromosome 7H harbored two loci associated with marker SCRI_RS_159555.

Table 5. Regions harboring QTLs for studied traits with the names of the nearest SNP markers

| name of hotspo | Trait | QTL ID | Chromosome | Position (cM) | Nearest marker |
|---|---|---|---|---|---|
| A | NSS | QNSS.IPG-1H_1 | 1H | 0,00 | BOPA1_4625-1413 |
| | NGS | QNGS.IPG-1H_ | 1H | 0,00 | BOPA1_4625-1413 |
| | LS | QLS.IPG-1H | 1H | 0,00 | BOPA1_4625-1413 |
| | LSt | QLSt.IPG-1H | 1H | 0,00 | BOPA1_4625-1413 |
| | GY | QGY.IPG-1H | 1H | 0,00 | BOPA1_4625-1413 |
| B | LS | QLS.IPG-2H | 2H | 21,00 | BK_13 |
| | LSt | QLSt.IPG-2H_1 | 2H | 21,00 | BK_13 |
| | NSS | QNSS.IPG-2H_1 | 2H | 22,00 | BK_12 |
| | NGS | QNGS.IPG-2H | 2H | 22,00 | BK_12 |
| | Density | QDen.IPG-2H_1 | 2H | 22,00 | BK_12 |
| | GWS | QGWS.IPG-2H_ | 2H | 22,00 | BK_12 |
| | GY | QGY.IPG-2H | 2H | 22,00 | BK_12 |
| | HD | QHD.IPG-2H | 2H | 22,00 | BK_12 |
| | HLKw | QHLKw.IPG-2H | 2H | 22,00 | BK_12 |
| | FHBi | QFHB.IPG-2H_ | 2H | 23,10 | BOPA1_5880-2547 |
| C | Density | QDen.IPG-2H_3 | 2H | 225,26 | BOPA2_12_10937 |
| | LSt | QLSt.IPG-2H_2 | 2H | 225,26 | BOPA2_12_10937 |
| | GWS | QGWS.IPG-2H_ | 2H | 228,70 | BOPA2_12_10937 |
| | TGW | QTGW.IPG-2H_ | 2H | 228,70 | BOPA2_12_10937 |
| | NSS | QNSS.IPG-2H_2 | 2H | 229,80 | SCRI_RS_174051 |
| D | TGW | QTGW.IPG-4H_ | 4H | 127,40 | BOPA1_2196-195 |
| | GWS | QGWS.IPG-4H_ | 4H | 127,40 | BOPA1_2196-195 |
| E | Density | QDen.IPG-5H_1 | 5H | 93,90 | SCRI_RS_184066 |
| | FHBi | QFHB.IPG-5H | 5H | 95,60 | SCRI_RS_184066 |
| | NGS | QNGS.IPG-5H_ | 5H | 97,30 | BOPA2_12_30929 |
| | LSt | QLSt.IPG-5H | 5H | 97,30 | BOPA2_12_30929 |
| | LS | QLS.IPG-5H | 5H | 97,30 | BOPA2_12_30929 |
| | NSS | QNSS.IPG-5H_1 | 5H | 98,67 | SCRI_RS_235055 |
| F | GY | QGY.IPG-5H | 5H | 285,20 | BOPA2_12_30533 |
| | NSS | QNSS.IPG-5H_2 | 5H | 286,90 | SCRI_RS_206867 |
| | NGS | QNGS.IPG-5H_2 | 5H | 286,90 | SCRI_RS_206867 |
| | HLKn | QHLKn.IPG-5H | 5H | 288,00 | SCRI_RS_165919 |
| G | GWS | QGWS.IPG-7H_ | 7H | 119,80 | SCRI_RS_159555 |
| | TGW | QTGW.IPG-7H_ | 7H | 119,80 | SCRI_RS_159555 |

Fig 4. Locations of regions (A – chromosome 1H and B,C – chromosome 2H) harboring QTLs detected for studied traits in the LCam population. Ppd-H1 gene localisation and corresponding markers were shown. Genetic distance scale in centiMorgan (cM) is place in the left margin.

An overrepresentation analysis was performed to identify enriched Gene Ontology (GO) terms – cellular component, molecular function and biological process - associated with regions

462 listed in Table 5, containing QTLs connected to FHB. There are multiple genes that are in the
463 regions - hotspot associated with traits analyzed in this study. Based on gene annotation and
464 literature studies, selected candidate genes related to disease resistance were shown in Table 6.

465

466 Table 6. Selected candidate genes identified by using the Barleymap database
467 (http://floresta.eead.csic.es/barleymap).

| Hotspot name | Marker | chr | Gene class | Description |
|---|---|---|---|---|
| B | HORVU2Hr1G013390 | chr2H | HC_G | UDP-Glycosyltransferase superfamily protein |
| | HORVU2Hr1G013400 | chr2H | HC_G | pseudo-response regulator 7 |
| | HORVU2Hr1G013590 | chr2H | HC_G | Glycosyltransferase |
| | HORVU2Hr1G013630 | chr2H | HC_G | Glycosyltransferase |
| | HORVU2Hr1G014020 | chr2H | HC_G | Jasmonate-induced protein |
| | HORVU2Hr1G014050 | chr2H | HC_G | 26S protease regulatory subunit 6B homolog |
| | HORVU2Hr1G014060 | chr2H | HC_G | 26S protease regulatory subunit 6B |
| | HORVU2Hr1G014080 | chr2H | HC_G | 26S protease regulatory subunit 6B homolog |
| | HORVU2Hr1G014440 | chr2H | HC_G | ubiquitin-activating enzyme 1 |
| | HORVU2Hr1G014500 | chr2H | HC_G | Pathogenesis-related protein 1-8 |
| | HORVU2Hr1G014770 | chr2H | HC_G | 26S protease regulatory subunit 4 homolog |
| E | HORVU5Hr1G095010 | chr5H | HC_G | UDP-Glycosyltransferase superfamily protein |
| | HORVU5Hr1G096210 | chr5H | HC_G | UDP-Glycosyltransferase superfamily protein |
| | HORVU5Hr1G096230 | chr5H | HC_G | UDP-Glycosyltransferase superfamily protein |
| | HORVU5Hr1G096240 | chr5H | HC_G | UDP-Glycosyltransferase superfamily protein |
| | HORVU5Hr1G096260 | chr5H | HC_G | UDP-Glycosyltransferase superfamily protein |
| | HORVU5Hr1G096310 | chr5H | HC_G | UDP-Glycosyltransferase superfamily protein |
| | HORVU5Hr1G096320 | chr5H | HC_G | UDP-Glycosyltransferase superfamily protein |
| | HORVU5Hr1G096340 | chr5H | HC_G | UDP-Glycosyltransferase superfamily protein |
| | HORVU5Hr1G096360 | chr5H | HC_G | UDP-Glycosyltransferase superfamily protein |
| | HORVU5Hr1G095350 | chr5H | HC_G | Glucan endo-1,3-beta-glucosidase 11 |
| | HORVU5Hr1G095380 | chr5H | HC_G | Glucan endo-1,3-beta-glucosidase 11 |
| | HORVU5Hr1G095420 | chr5H | HC_G | Glucan endo-1,3-beta-glucosidase 7 |
| F | HORVU5Hr1G071810 | chr5H | HC_G | Auxin response factor 10 |
| | HORVU5Hr1G071940 | chr5H | HC_G | UDP-Glycosyltransferase superfamily protein |
| | HORVU5Hr1G073630 | chr5H | HC_G | Auxin efflux carrier family protein |
| | HORVU5Hr1G073670 | chr5H | HC_G | Auxin efflux carrier family protein |

468
469
470
471
472
473
474

## Discussion

It is widely known that a mapping population derived from parents divergent in genetic composition allows high performance QTL analysis. In this study, RILs (named LCam) derived from a European variety and a Syrian breeding line were used for QTL analysis. Both parental forms were differentiated in terms of stature, grain yield, HD and resistance/tolerance to biotic and abiotic stresses [37, 38]. CamB is unadapted to the Central Europe region and has undesired agonomical trats such as early heading and tall stature. Lubuski is an old cultivar with agro-morphological-physiological characters adapted to Polish climatic conditions during a long cultivation period. With the aim of providing the genetic variability between the parents of the mapping populaion and increasing the chance to indentifying loci linked to FHB we conducted field experiments using RILs derived from a cross between Lubuski and CamB genotypes.

FHB, caused by *Fusarium culmorum*, is a very important disease of crops globally [9]. Damage caused by *Fusarium* species fungus includes reduced grain yield, and reduced grain functional quality, and results in the presence of the mycotoxin deoxynivalenol in FDK (and also in grains without any visible symptoms). The development of FHB resistant crop cultivars is an important component of integrated breeding management [54, 55]. The objective of this investigation was to identify QTLs for traits linked to yield performance in a recombinant inbred line population grown under a disease-free environment and under *Fusarium* infection conditions.

FHB infection can be evaluated in different ways. In field conditions, FHB can be determited, among others, by visual inspection of the percentage of infected spikelets [56]. This percentages can be used to determine an FHB index [57]. In this study, different tools were employed to estimate disease severity: FHBi was calculated as: (spike infection in % percentage of spikelets affected within a spike) / (percentage of infected spikes per plot). After harvest, percentage both FDK and HLK as described by the visual symptom score of the kernels and the weight of the kernels were evaluated. In addition, DON concentration was quantified.

In this study Lubuski was less susceptible to FHB than Syrian parent in all type of conditions in terms of DON accumulation. On the other hand, we observed a higher FHBi value for Lubuski plants in infection conditions. DON tests of grains harvested from the LCam population showed that some RILs showed lower DON content values than CamB, while some other RILs were more susceptible than Lubuski. In all types of conditions, the mean values of agronomic traits performed as expected – biotic stress conditions impaired yields. In control conditions, DON contamination represents the natural occurrence of FHB [58] and the level of mycotoxin accumulation varied significantly from the ones observed in LCam plants grown in infection conditions.

Most of the correlation coefficients among the FHBi and other studied characters were negative an statistically different from zero ($P<0.01$). The Pearson correlation coefficient was also significantly negative between FHBi and the two main traits of our interest – HD and LSt, which is in agreement with previous studies [59–61], where plants with lower FHB severities have usually been characterized by late heading and tall stature. Late-maturing plants may head during a time in the summer less suitable for infection, and tall plants avoid higher concentrations of inoculum near the surface of the soil [62]. Another study, conducted by Mesfin et al. [24] concluded that late HD may be linked to FHB resistance since the heads experience less exposure time to fungal spores.

Visual ratings for FHB in barley plants are usually conducted just before the spikes begin to lose chlorophyll so disease symptoms can be easily counted. In some years, there are favorable conditions for *Fusarium* growth and DON accumulation throughout plant senescence, reducing correlations between FHB and DON because the FHB score does not accurately reflect the final disease level [63]. It is well known that symptomless spikes can be contaminated with DON [64]. Traditionally, mycotoxin determination has mainly been performed by chromatographic techniques [65, 66]. ELISA has been proposed as an alternative method to visual scoring and DON

526 quantification for mesuring FHB [67] (Hill et al. 2008). Expression of DON by fungal myceium
527 is environmentally dependent [68], whereas the expression of monoclonal antibody-specific
528 mycelial proteins is not [69]. In consequence, ELISA and DON values are not always closely
529 correlated. In our study, no correlation was found between FHBi and DON level content, which
530 can be explained by this phenomenon.

531 Agronomic traits related to spike characters (e.g., spike density and sterility) have been
532 reported to be linked to FHB resistance but the association between the traits and FHB
533 vulnerability seems to be unclear. Steffenson et al. [70] reported that FHB severity was apparently
534 higher in dense spike NILs than in lax spikes. A negative correlation between FHB severity and
535 spike density has been recorded in an experiment conducted on a population derived from two-
536 row and six-row barley plants [71]. In contrast, in the study conducted by Yoshida et al. [72] on
537 barley NILs spike density had little or no effect. Ma et al. [73] also reported an association between
538 lax spike and FHB reaction. Lax spikes may be related to FHB resistance due to their specific
539 architecture that retains, presumably, less moisture within the whole spike. This decreases the pace
540 of fungus spread [4]. In the presented study negative correlations were detected between the traits
541 Density and FHBi, indicating that spike compactness may be one of the factors enhancing FHB
542 susceptibility. A positive correlation was recorded between Sterility and FHBi for LCam plants,
543 which means that FHB infection has negative effects on seed development, as expected.

544 Single nucleotide polymorphisms (SNPs) that are widely distributed throughout the
545 genome have been used in QTL mapping [74, 75]. In our previous study using 1536 SNP markers,
546 we developed genetic map which allowed us to identify a set of QTLs linked to different agronomic
547 traits (among others: HD and plant height) in field [38] and greenhouse conditions [37]. In this
548 study, by using a 9K SNP array, we improved the QTL mapping resolution due to increased marker
549 density.

The SNP markers were distributed across all seven linkage groups in the LCam mapping population. Marker order and distances for SNPs generally matched previously published barley maps [40, 76]. The genetic map consisting of 1947 SNPs which has been developed in this investigation, covering 1678 cM, is larger than other maps (e.g., constructed by Wang et al. [77] − 1375.8 cM.

Many bi-parental mapping studies have been conducted on barley to explain the genetic architecture of resistance to FHB and DON accumulation and to identify molecular markers that could be useful in breeding [24, 31, 78, 79]. FHB resistance has frequently been found to be associated with plant morphology parameters, especially plant height, spike architecture, anther extrusion and HD acting mainly as passive resistance factors. For this reason, the LCam population was also evaluated for HD, plant height, spike compactness and other traits, which seem to be important form an agronomic point of view. Numerous QTL mapping studies that have been conducted in different crop species have revealed that QTLs associated with FHB resistance are coincident with QTLs linked to various agronomic and morphological traits [4, 24, 79]. In our investigation, a set of 70 QTLs were detected in seven barley chromosomes. A higher number of QTLs for agronomic traits was found on chromosome 2H, where the greatest number of FHB-linked QTLs was also identified.

QTLs for FHB resistance have been found on all seven barley chromosomes [24, 31, 78–81]. For most of the resistance varieties, QTLs associated with FHB were detected on the long arm of chromosome 2H [30, 31, 82]. In addition, QTLs for disease resistance and reduced DON concentration have been linked to spike morphology controlled by *vrs1* and a major HD locus (P*pd-H1*) in numerous studies [80]. The number of detected QTLs varies depending on the type of research, ranging from only one in the study conducted by Mesfin et al. [24] to two [4, 31, 73] or even to 10 QTLs [22]. For many FHB regions in the barley genome, QTLs for DON concentration have been detected both for barley [81, 82] and for wheat [83, 84] but this kind of

575 coincidence has not been reported as significant in all studies [30]. Identification of QTLs linked
576 to FHB symptoms has been confounded by agronomic characters such as HD, plant height or
577 properties associated with spike morphology [24, 79]. Hence, mapping of traits characterized by
578 strong phenotypic correlations constitutes a challenge in terms of pleiotropy/linkage. Massman et
579 al. [80] have summarized previously described FHB regions and showed all detected QTLs in a
580 graph associated with genome location (bin). The QTLs were located on chromosome 2H at three
581 different spots (bin 8, bin 10 and bin 13-14). In our investigation, six QTLs related do FHBi were
582 found. Out of these QTLs, three were identified on chromosome 2H at position 23.1, 87.7 and
583 216.7 cM corresponding to previously mentioned bin locations. Three other loci: QFHB.IPG-3H,
584 QFHB.IPG-5H and QFHB.IPG-7H were found on chromosomes 3H, 5H and 7H, respectively.
585 QFHB.IPG-2H_1 was found on the short arm of chromosome 2H in the vicinity of SNP marker
586 BOPA1_5880-2547 and this explains the largest percentage of phenotyping variance (3.69 –
587 30.69) of all detected FHB QTLs. The Syrian parent alleles positively contributed to the increase
588 in FHBi at this locus, which is in accordance with previous studies, in which early heading plants
589 were vulnerable to FHB symptoms. In our study, the main QTL for HD was located on
590 chromosome 2H in the vicinity of marker BK_12 at position 22 cM, shifted 1.1 cM from marker
591 BOPA1_5880-2547. According to Turner at al. [85] the most significant SNP marker (BK_12) is
592 directly located within the *Ppd-H1* gene, which is the main determinant of response to long day
593 conditions in barley. The 2Hb8 QTL is also considered a major locus for resistance to FHB and
594 DON accumulation [86]. Delayed head emergence may increase the likelihood that the host will
595 escape infection by the pathogen [71, 87]. On the other hand, late heading is undesirable in
596 breeding programs addressed to arid regions [88]. Plants with lower FHB severities usually have
597 one or more of the following traits: late heading, increased height and two-rowed spike
598 morphology [59, 60, 70]. Although tall plants are usually more resistant to disease than short plant
599 [73], heading date can be either negatively [71, 73] or positively correlated with DON content in

the seeds [22, 24]. The main QTL associated with heading and located on chromosome 2H (Q.HD.LC-2H), was also identified at SNP marker 5880–2547, in our previous study [37]. SNP 5880–2547 was the closest marker to QTLs associated with plant architecture, spike morphology and grain yield in the mentioned experiment. None of the detected QTLs for FHBi in the current study were classified as major loci (the heighest value of LogP value was 8.14 recorded for QFHB.IPG-2H_3), but this could be explained by the fact that the identification of many minor QTLs associated with the model of complex traits that predicts an exponential decay of QTL effects only a few loci but has large effects [89].

Plant height is under polygenic control and represents one of the most important agronomic traits for barley [90, 91]. The right timing of flowering time allows optimal grain development with regard to the availability of heat, light and water, while semi-dwarf cereals allocate more resources into grain production tan taller plants and show reduced losses through lodging [92, 93]. In addition, due to increasing of moisture content of the plants, lodging causes the infection expansion [94]. In the current study were detected seven loci for LSt. The main locus (QLSt.IPG-2H_1) was detected on chromosome 2H in the vicinity of marker BK_13, which coincided with the main HD QTL. In this study only one locus was found on chromosome 3H, where *sdw1/denso* has been located in our previous investigations [38, 90, 95]. There is a gradient at ascospore concentration from the soil surface to upper part of plant stem. Thus, short plant tend to have higher FHB infection level [96], which is in accordance with our results.

In barley, spike length and spike characters like number of grains and spikelets per spike are perceived as an important agromorphological traits due a direct impact on crop yield [97]. The spike architecture has significant influence on yield and might alter the spike microenvironment making it less favorable for fungal infection [98]. In the current study six QTLs linked to Density were found. Out of six detected QTLs, four loci were found on chromosome 2H. The major QTL (QDen.IPG-2H-1) was located on the short arm of 2H in the vicinity of marker BK_12. Two QTLs

625 related to the density of the spike were found on chromosome 5H. In most cases CamB alleles
626 contributed positively to this trait. In many studies plants with lax spikes have been reported as
627 less vulnerable for fungal infection [82, 98]. On the other hand, Yoshida et al. [62] found no
628 differences between genotypes when compared barleys with normal and dense type of spike.
629 Steffenson et al. [70] showed that FHB severity was higher in dense spike NILs than in lax spike
630 plants but no significant differences were found. Langevin et al. [99], conducting the study using
631 barley with two- and six-row type of spike, concluded that the high level of DON contamination
632 observed among dense spikes accured mainly because of direct contact of the florets. To
633 summarize, results for the association between disease severity and spike architecture of the barley
634 plants are not consistent.

635 The genes encoding UDP-Glycosyltransferase superfamily protein were found for all
636 hotspots containing QTLs linked to FHB (FHBi, HLKn, HLKw). Plant uridine diphosphate
637 (UDP)-glucosyltransferases (UGT) catalyze the glucosylation of xenobiotic, endogenous
638 substrates and phytotoxic agents produced by pathogens such as mycotoxins [100, 101]. The
639 studies have shown that plant UDP-glucosyltransferase genes have significant role in plant
640 resistance both to biotic and abiotic stresses [102, 103]. Poppenberger et al. [104] demonstrated
641 that DON resistance can be achieved by the enzymatic conversation (a natural detoxification
642 process in plants called glycosylation) of the toxin into the non-toxic form (DON-3-0-glucoside)
643 by UDP-glucosyltransferase. It is also worth to mention that in our study 10 records have been
644 annotated for region E, where FHBi QTL was found on chromosome 5H. Recently the HvUGT-
645 10 W1 gene has been isolated from an FHB resistant barley variety conferred FHB tolerance [102].

646 Region B, as tightly linked to the QTLs identified for FHBi and HD in this study, has been
647 annotated also as pathogenesis-related protein 1-8 (HORVU2Hr1G014500). These type of
648 proteins belong to the antimicrobial compounds playing an important role in defense response
649 against fungal infection. Induction of PR (Pathogen-related)- proteins has been found in many

650 plant species belonging to various families [105]. For instance, Pritsch et al. [106] observed that
651 the transcripts of defense response genes, peroxidase and PR-1 to -5, accumulated as early as 6 to
652 12 h after wheat spikes were inoculated with *F. graminearum*.

653 Another gene annotation linked to disease resistance was shown for region B. Glucan endo-
654 1,3-beta-glucosidase may provide a degree of protection against microbial invasion of germinated
655 barley grain through its ability to degrade fungal cell wall polysaccharides, according to
656 Balasubramanian et al. [107].

657 Data obtained from Barley Map Floresta database allowed us to annotate both in region F
658 and B candidate genes related to two types of phytohormones, which play pivotal roles in
659 regulation of this defence network [108]. Several regions identified in our analysis included
660 annotations associated with auxin (HORVU5Hr1G071810 - auxin response factor 10;
661 HORVU5Hr1G073630, chr5H, HORVU5Hr1G073670 - auxin efflux carrier family protein) in
662 region F. The roles of auxins in plant-pathogen interactions have also been described in recent
663 years [109, 110]. Another phytohormone annotation (jasmonate-induced protein) was present in
664 the region B. Jasmonic acid (JA) is considered to be a critical phytohormone for plant defense
665 response against pathogens [111]. For instance, Gottwald et al. [112] suggested that Jasmonate
666 and ethylene dependent defense and suppression of fungal virulence factors are major mechanisms
667 of FHB resistance in wheat.

668 In the region B were found also following annotations:pseudo-response regulator 7
669 (HORVU2Hr1G013400), 26S protease regulatory subunit 6B (HORVU2Hr1G014050,
670 HORVU2Hr1G014060 and HORVU2Hr1G014080) and ubiquitin-activating enzyme 1
671 (HORVU2Hr1G014440). All these annotations are linked to *HvPpd-H1*, which provides
672 adaptation to photoperiod in barley. The barley Ppd-H1 gene is homologous to Arabidopsis
673 PRR3/PRR7 and mediates the acceleration of development in long-days [113]. The Ppd-
674 H1/PRR37 allele is the major determinant of photoperiod response in barley and is the putative

675 AtPRR7 orthologue [85]. Proteasomes are involved in the degradation of ubiquitin-tagged
676 proteins. Alterations in proteasome subunits were found in several proteomic studies dealing with
677 both abiotic and biotic stresses [114, 115].

678 Ubiquitin is well established as the major modifier of signaling in eukaryotes. The main
679 characteristic of ubiquitination is the conjugation of ubiquitin onto lysine residues of acceptor
680 proteins [116]. In most cases, the targeted protein is degraded by the 26S proteasome, the major
681 proteolysis machinery in eukaryotic cells. The ubiquitin– proteasome system is responsible for
682 removing most abnormal peptides and short-lived cellular regulators. This allows cells to respond
683 rapidly to intracellular signals and changing environmental conditions. In our study, annotations
684 linked to 26S protease regulatory subunits were found in region B (HORVU2Hr1G014050,
685 HORVU2Hr1G014060, HORVU2Hr1G014080 and HORVU2Hr1G014770).

686

687

688 Conclusions

689

690 Results from the research conducted recently have revealed that most of the resistant barley
691 genotypes showed QTL linked to FHB on the long arm of 2H chromosome, the first a coincident
692 QTL for HD and the second associated with *vrs1* gene. In our study, two major QTLs (QFHB.IPG-
693 2H_1 and QFHB.IPG-2H_2) found on chromosome 2H were located in the similar positions as
694 the loci detected in previus studies (30, 86). A major confounding problem in mapping loci for
695 FHB resistance is that QTLs for the agromorphological traits (HD, length of stem and spike type)
696 are often coincident with the loci for disease resistance and they may interfere with resistance
697 evaluation [82, 83]. Furthermore, it can be difficult to reveal the genetic architecture of these
698 traits (linked QTL or pleiotropy) when many QTL are identified at the same locus. On the other
699 hand, our results support a major assumption that plant architecture and inflorescence traits are
700 associated significantly with FHB severity.

Out of six detected FHB QTLs in the current study, four were not classified as a loci localisated in the hotspots, where many yield-related loci were detected. Although, in previously conducted studies QTLs associated with FHB were found on chromosomes 3H, 5H and 7H, QTLs identified in our investigation appear to be unique for FHB symptoms. Thus, the barley genotypes carrying these QTLs may be used in breeding programs without the confounding effects from another yield-related traits.

## Supporting Information

S1 Table. The mean values for studied traits for parental cultivars.
(DOC)
S2 Table. The mean values for studied traits for RILs.
(DOC)
S3 Table . QTLs identified in the LCam population for the observed traits.
(DOC)

## Acknowledgments

This work was financially supported by Polish Ministry of Agriculture and Rural Development (grant no HOR hn-501-19/15 Task 88).

## Author Contributions

PO, AK, KM conception and design of the study; AK funding acquisition, project coordination; PO, MK, MR, DJ plant breeding and stresses application; MK, PO, KM, AK sampling of plant material; PK, HĆK methodology validation, statistics and computations; PO, AK, KM, MK, DJ samples preparation, laboratory work and analyses; PO, AK, KM, TA, MS, PK data analysis and interpretation, manuscript writing, revision and editing; PO, AK, KM, MK, TA, MS, PK, HĆK, MR and DJ contributed to the final version of the manuscript.

## References

1. Bottalico A, Perrone G. Toxigenic Fusarium species and mycotoxins associated with head blight in small-cereals in Europe. Eur J Plant Pathol. 2002;08: 611–624.
2. Shi W, Tan Y, Wang S, Gardiner MD, De Saeger S, Liao Y et al. Mycotoxigenic potentials of Fusarium species in various culture matrices revealed by mycotoxin profiling. Toxins. 2017; 9: 6–21.
3. Berger G, Green A, Khatibi P, Brooks W, Rosso L, Liu S, et al. 2014. Characterization of Fusarium Head Blight Resistance and Deoxynivalenol Accumulation in Hulled and Hulless Winter Barley. Plant Disease. 2014;98: 599–606.
4. Zhu et al. 1999. Zhu H, Gilchrist L, Hayes P, Kleinhofs A, Kudrna D, Liu Z, et al. 1999. Does function follow form? Principal QTLs for Fusarium head blight (FHB) resistance are coincident

with QTLs for inflorescence traits and plant height in a doubled-haploid population of barley. Theor Appl Genet. 1999; 99:1221–1232.

5. European Food Safety Authority (EFSA). Risks to human and animal health related to the presence of deoxynivalenol and its acetylated and modified forms in food and feed. EFSA Journal. 2017;15: 4718.
6. Sobrova P, Adam V, Vasatkova A, Beklova M, Zeman L, Kizek R. 2010. Deoxynivalenol and its toxicity. Interdiscip Toxicol. 2010;3: 94–99.
7. Bernhoft A, Torp M, Clasen PE, Løes AK, Kristoffersen AB. Influence of agronomic and climatic factors on Fusarium infestation and mycotoxin contamination of cereals in Norway. Food Addit Contam A. 2012;29: 1129–1140.
8. Schöneberg T, Musa T, Forrer H-R, Mascher F, Bucheli TD, Bertossa M, et al. Infection conditions of Fusarium graminearum in barley are variety specific and different from those in wheat Eur J Plant Pathol. 2018;151: 975–989.
9. Wiśniewska H, Surma M, Krystkowiak K, Adamski T, Kuczyńska A, Ogrodowicz P, et al. Simultaneous selection for yield-related traits and susceptibility to Fusarium head blight in spring wheat RIL population. Breeding Sci. 2016;66: 281–292.
10. Alshannaq A, Yu JH. Occurrence, toxicity, and analysis of major mycotoxins in food. Int J Environ Res Public Health. 2017;p.632.
11. Levasseur-Garcia C. UpdatedOverview of Infrared Spectroscopy Methods for Detecting Mycotoxins on Cereals (Corn,Wheat, and Barley). Toxins. 2018;10: 3.
12. Ji F, Li H, Xu JH, Shi JR. Enzyme-linked immunosorbent-assay for deoxynivalenol (DON). Toxins. 2011;3: 968–978. doi: 10.3390/toxins3080968.
13. Eslami M, Mashak Z, Heshmati A, Shokrzadeh M, Sasan A, Nejad M. Determination of aflatoxin B1 levels in Iranian rice by ELISA method. Toxin Rev. 2015;34: 125–128. doi: 10.3109/15569543.2015.1074925.
14. Cai X, Xu S, Oliver R, Zhang Q, Stack R, Zhong S, et al. Alien introgression for FHB resistance in wheat – challenges and strategies. In: Appels R, Eastwood R, Lagudah E, Langridge P, Mackay M, McIntyre L, Sharp P, editors. Proceedings of the 11th International Wheat Genet Symposium; Aug 24–29; Brisbane, Qld, Australia: Sydney Univ Press, Sydney (Australia); 2008.
15. Buerstmayr M, Huber K, Heckmann J, Steiner B, Nelson J, Buerstmayr H. Mapping of QTL for Fusarium head blight resistance and morphological and developmental traits in three backcross populations derived from Triticum dicoccum × Triticum durum. Theor Appl Genet. 2012;125: 1751–1765. doi: 10.1007/s00122-012-1951-2.
16. Schulte D, Close TJ, Graner A, Langridge P, Matsumoto T, Muehlbauer G, et al. The international barley sequencing consortium—at the threshold of efficient access to the barley genome. Plant Physiol. 2009;149: 142–147.
17. Hunt CW. Factors affecting the feeding quality of barley for ruminants. Anim Feed Sci Technol. 1996;62: 37–48.
18. Ullrich SE, Han F, Froseth JA, Jones BL, Newman CW, Wesenberg DM. Mapping of loci affect carbonhydrate content inbarley grain. In: Proceedings of V International Oat Conference & VII Bar-ley Genetic Symposium, Saskatoon; 30 July – 6 August 1993. pp.141–143.
19. Saisho D, Takeda K. Barley: emergence as a new research material of crop science. Plant Cell Physiol. 2011;52(5): 724–727.
20. Savi, GD, Piacentini KC, Tibola C, Scussel VM. (2014). Mycoflora and deoxynivalenol in whole wheat grains (Triticum aestivum) from Southern Brazil. Food Addit Contam Part B Surveill. 2014;7(3): 232–7. doi: 10.1080/19393210.2014.898337.
21. Steffenson BJ. "Fusarium head blight of barley: impact, epidemics, management, and strategies for identifying and utilizing genetic resistance," in Fusarium Head Blight of Wheat and Barley, eds Leonard K. J., Bushnell W. R., editors. (Saint Paul, MN: The American Phytopathological Society); 2003. 241–295.

22. de la Pena KP, Smith F, Capettini GJ, Muehlbauer M, Gallo-Meagher R, et al. Quantitative trait loci associated with resistance to Fusarium head blight and kernel discoloration in barley Theor Appl Genet. 1999;99: 561–569.
23. Ma ZQ, Zhao DM, Zhang CQ, Zhang ZZ, Xue SL, Lin F, Kong ZX, Tian DG, Luo QY. Molecular genetic analysis of five spike-related traits in wheat using RIL and immortalized F-2 populations. Mol. Genet. Genomics. 2007;277(1): 31–42.
24. Mesfin A, Smith KP, Dill-Macky R, Evans CK, Waugh R, Gustus CD, et al. Quantitative trait loci for Fusarium head blight resistance in barley detected in a two-rowed by six-rowed population. Crop Sci. 2003;43: 307–318. doi: 10.2135/cropsci2003.3070.
25. Geddes J, Eudes F, Laroche A, Selinger LB. Differential expression of proteins in response to the interaction between the pathogen Fusarium graminearum and its host, Hordeum vulgare. Proteomics. 2008;8: 545–554.
26. Mesterhazy A. Types and components of resistance to Fusarium head blight of wheat. Plant Breed. 1995;114: 377–386. doi: 10.1111/j.1439-0523.1995.tb00816.x.
27. Bai G, Shaner G. Scab of wheat: prospects for control. Plant Dis. 1994;78: 760–766.
28. Zhao L, Ma X, Su P, Ge W, Wu H, Guo X, et al. Cloning and characterization of a specific UDP-glycosyltransferase gene induced by DON and Fusarium graminearum. Plant Cell Rep. 2018; 37(4): 641–652. doi: 10.1007/s00299-018-2257-x.
29. Yu JB, Bai GH, Zhou WC, Dong YH, Kolb FL. Quantitative trait loci for Fusarium head blight resistance in a recombinant inbred population of Wangshuibai/Wheaton. Phytopathology. 2008;98: 87–94.
30. Dahleen LS, Morgan W, Mittal S, Bregitzer P, Brown RH, Hill NS. Quantitative trait loci (QTL) for Fusarium ELISA compared to QTL for Fusarium head blight resistance and deoxyniva-lenol content in barley. Plant Breed. 2012;131: 237–243. doi:10.1111/j.1439-0523.2012.01952.x.
31. Dahleen L, H. Agrama H, R. Horsley R, B. Steffenson B, P. Schwarz P, A. Mesfin A, et al. Identification of QTLs associated with Fusarium head blight resistance in Zhedar 2 barley. Theor Appl Genet. 2003;108: 95–104. doi:10.1007/s00122-003-1409-7.
32. Buerstmayr M, Lemmens M, Steiner B, Buerstmayr H. Advanced backcross QTL mapping of resistance to Fusarium head blight and plant morphological traits in a Triticum macha × T. aestivum population. Theor Appl Genet. 2011;123: 293–306. doi: 10.1007/s00122-011-1584-x.
33. Mao S, Wei Y, Cao W, Lan X, Yu M. Confirmation of the relationship between plant height and Fusarium head blight resistance in wheat (Triticum aestivum L.) by QTL meta-analysis. Euphytica. 2010;174: 343–356. doi: 10.1007/s10681-010-0128-9.
34. Rostoks N, Ramsay L, MacKenzie K, Cardle L, Bhat PR, Roose ML, et al. (2006) Recent history of artificial outcrossing facilitates whole-genome association mapping in elite inbred crop varieties. Proc Natl Acad Sci. 2006;103(49): 18656–1866. doi.org/10.1073/pnas.0606133103.
35. Waugh R, Jannink JL, Muehlbauer GJ, Ramsay L. The emergence of whole genome association scans in barley. Curr Opin Plant Biol. 2009;12: 218–222.
36. Comadran J, Kilian B, Russell J, Ramsay L, Stein N, Ganal M, et al. Natural variation in a homolog of Antirrhinum CENTRORADIALIS contributed to spring growth habit and environmental adaptation in cultivated barley. Nat Genet. 2012;44: 1388–1392. doi: 10.1038/ng.2447.
37. Ogrodowicz P, Adamski T, Mikołajczak K, Kuczyńska A, Surma M, Krajewski P, et al. QTLs for earliness and yield-forming traits in the Lubuski × CamB barley RIL population under various water regimes. J Appl Genet. 2017;58: 49–65. doi: 10.1007/s13353-016-0363-4.
38. Mikołajczak K, Ogrodowicz P, Gudyś K, Krystkowiak K, Sawikowska A, Frohmberg W, et al. Quantitative trait loci for yield and yield–related traits in spring barley populations derived from crosses between European and Syrian cultivars. PLoS ONE. 2016;11(5): e0155938. doi: 10.1371/journal.pone.0155938.

844 39. Close TJ, Bhat PR, Lonardi S, Wu Y, Rostoks N, Ramsay L, et al. Development and
845 implementation of high-throughput SNP genotyping in barley. BMC Genomics. 2009;10: 582.
846 doi: 10.1186/1471-2164-10-582.
847 40. Muñoz-Amatriaín M, Moscou MJ, Bhat PR, Svensson JT, Bartoš J, Suchánková P et al. An
848 improved consensus linkage map of barley based on flow-sorted chromosomes and single
849 nucleotide polymorphism markers. Plant Genome. 2011;4: 238–249.
850 41. Bayer MM, Rapazote-Flores P, Ganal M, Hedley PE, Macaulay M, Plieske J, et al. Development
851 and evaluation of a barley 50k iSelect SNP array. Front Plant Sci. 2017;8: 1792. doi:
852 10.3389/fpls.2017.01792
853 42. Van Ooijen J. JoinMap 4. Software for the calculation of genetic linkage maps in experimental
854 populations. Wageningen: Kyazma BV; 2006.
855 43. Malosetti M, Ribaut J-M, van Eeuwijk FA. The statistical analysis of multi-environment data:
856 modeling genotype-by-environment interaction and its genetic basis. Front Physiol. 2013;4: 44.
857 doi: 10.3389/fphys.2013.00044.
858 44. Li J, Ji L. Adjusting multiple testing in multilocus analyses using the eigenvalues of a correlation
859 matrix. Heredity. 2005;95: 221–227. doi: 10.1038/sj.hdy.6800717.
860 45. VSN International. GenStat for Windows 16th Edition VSN International. Hemel Hempstead;
861 2013.
862 46. Rant JC, Arraiano LS, Chabannes M, Brown JKM. Quantitative trait loci for partial resistance
863 to Pseudomonas syringae pv. maculicola in Arabidopsis thaliana. Mol Plant Pathol. 2013;14:
864 828–837. doi: 10.1111/mpp.12043.
865 47. Dhariwal R, Fedak G, Dion Y, Pozniak C, Laroche A, Eudes F, et al. High density single
866 nucleotide polymorphism (SNP) mapping and quantitative trait loci (QTL) analysis in a
867 biparental spring triticale population localized major and minor effect Fusarium head blight
868 resistance and associated traits QTL. Genes (Basel). 2018;9(1).
869 48. Saxena RK, Kale SM, Kumar V, Parupalli S, Joshi S, Singh VK, et al. Genotyping-by-
870 sequencing of three mapping populations for identification of candidate genomic regions for
871 resistance to sterility mosaic disease in pigeonpea. Sci Rep. 2017;7: 1813.
872 49. Gahlaut V, Jaiswal V, Tyagi BS, Singh G,Sareen S, Balyan HS, et al. (2017)QTL mapping for
873 nine drought-responsive agronomic traits in bread wheat under irrigated and rainfed
874 environments. PLoS ONE 12(8):e0182857. doi.org/10.1371/journal.pone.018285.
875 50. Cantalapiedra CP, Boudiar R, Casas MA, Igartua E, Contreras-Moreira B. BARLEYMAP:
876 physical and genetic mapping of nucleotide sequences and annotation of surrounding loci in
877 barley. Mol Breed. 2015;35: 13.
878 51. Lee JA, Sinkovits RS, Mock D, Rab EL, Cai J, Yang P et al. Components of the antigen
879 processing and presentation pathway revealed by gene expression microarray analysis following
880 B cell antigen receptor (BCR) stimulation. BMC Bioinformatics. 2006;2(7): 237.
881 52. Luo F, Yang Y, Chen CF, Chang R, Zhou J, Scheuermann RH, et al. Modular organization of
882 protein Interaction networks. Bioinformatics. 2007;23: 207–214.
883 53. Benjamini Y, Hochberg Y. Controlling the false discovery rate: a practical and powerful
884 approach to multiple hypothesis testing. J R Stat Soc. 1995;57: 289–300.
885 54. Surma M, Adamski T, Wiśniewska H, Kaczmarek Z, Mejza I, Mejza S, et al. Uni-and
886 multivariate approaches to evaluating the susceptibility of wheat hybrids to Fusarium head
887 blight. Czech J Genet Plant Breed. 2016;52: 132–138.
888 55. Shah L, Ali A, Yahya M, Zhu Y, Wang S, Si H, et al. Integrated control of fusarium head blight
889 and deoxynivalenol mycotoxin in wheat. Plant Pathol. 2018;67(3): 532–548.
890 56. Xue AG, Ho KM, Butler G, Vigier BJ, Babcock C. Pathogenicity of Fusarium species causing
891 head blight in barley. Phytoprotection. 2006;87: 55–61.
892 57. Tekauz A, McCallum B, Gilbert J. Review: fusarium head blight of barley in western Canada.
893 Can J Plant Pathol. 2000;22: 9–16.

58. Zhang JX, Jin Y, Rudd JC, Bockelman HE. New Fusarium head blight resistant spring wheat germplasm identified in the USDA National Small Grains Collection. Crop Sci. 2008; 48 (1): 223–235.
59. Parry DW, Jenkinson P, McLeod L. Fusarium ear blight(scab) in small-grain cereals—a review. Plant Pathol. 1995;44: 207–238.
60. Rudd JC, Horsley RD, McKendry AL, Elias EM. Host plantresistance genes for Fusarium head blight: sources, mechanisms, and utility in conventional breeding systems. Crop Sci. 2001;41: 620–627.
61. Huang Y, Haas M, Heinen S, Steffenson BJ, Smith KP, Muehlbauer GJ. QTL mapping of fusarium head blight and correlated agromorphological traits in an elite barley cultivar Rasmusson. Front Plant Sci. 2018;9: 1260. doi: 10.3389/fpls.2018.01260.
62. Yoshida M, Kawada N, Nakajima T. Effect of infectiontiming on Fusarium head blight and mycotoxin accumulation in open- and closed-flowering barley. Phytopathology. 2007;97: 1054–1062.
63. Paul PA, Lipps PE, Madden LV. 2005. Relationship between visual estimates of Fusarium head blight intensity and deoxynivalenol accumulation in harvested wheat grain: A meta-analysis. Phytopathology. 2005;95: 1225–1236.
64. Champeil A, Dore T, Fourbet JF. Fusarium head blight: epidemiological origin of the effects of cultural practices on head blight attacks and the production of mycotoxins by Fusarium in wheat grains. Plant Sci. 2004;166: 1389–1415.
65. Turner NW, Subrahmanyam S, Piletsky S. Analytical methods for determination of mycotoxins: a review. Anal Chim Acta. 2009;632: 168–180.
66. Pereira VL, Fernandes JO, Cunha SC. (2014) Mycotoxins in cereals and related foodstuffs: A review on occurrence and recent methods of analysis. Trends Food Sci Technol. 2014;36(2): 96–136.
67. Hill NS, Neate SM, Cooper B, Horsley R, Schwarz P, Dahleen LS, et al. 2008. Comparison of ELISA for Fusarium, visual screening, and deoxynivalenol analysis of Fusarium head blight for barley field nurseries. Crop Sci. 2008;48: 1389–1398.
68. Nita M, Tilley K, De Wolf E, Kuldau G. Effects of Moistureduring and after anthesis on the development of Fusarium head blight of wheat and mycotoxins production. In: Canty, S.M., Lewis, J., Siler,L. and Ward, R.W. (Eds.). In: Proceedings of the 2005 National Fusarium Head Blight Forum, HiltonMilwaukee City Center, Milwaukee, Wisconsin, USA; 2005. pp. 125–128.
69. Omori AM, Ono EYS, Hirozawa MT, de Souza Suguiura IM, Hirooka EY, Pelegrinelli Fungaro MH, et al. Development of Indirect Competitive Enzyme-Linked Immunosorbent Assay to Detect Fusarium verticillioides in Poultry Feed Samples. Toxins. 2019;11(1): E48. doi: 10.3390/toxins11010048.
70. Steffenson BJ, Prom LK, Salas B, Fetch TG, Wesenberg DM, Bockelman HE. "Severity of Fusarium head blight and concentrations of deoxynivalenol in near isogenic lines of barley differing for several agronomic characters," in Proceedings of the 7th International Barley Genetics Symposium, eds Slinkard A., Scoles G., Rossnagel B., editors. (Saskatoon: University Extension Press); 1996.
71. Urrea CA, Horsley RD, Steffenson BJ. Heritability of Fusarium head blight resistance and deoxynivalenol accumulation from barley accession. Crop Sci. 2002;42: 1404–1408.
72. Yoshida M, Kawada N, Tohnooka T. (2005) Effect of row type, flowering type and several other spike characters on resistance to Fusarium head blight in barley. Euphytica. 2005;141: 217–227.
73. Ma Z, Steffenson BJ, Prom LK, Lapitan NL. Mapping of quantitativetrait loci forFusariumhead blight resistance in barley. Phytopathology. 2000; 90(10): 1079–1088.

943 74. McCartney CA, Brûlé-Babel AL, Fedak G, Martin RA, Mccallum BD, Gilbert J, et al. (2016).
944 Fusarium head blight resistance QTL in the spring wheat cross Kenyon/86ISMN 2137. Front
945 Microbiol. 2016;7: 1542. doi: 10.3389/fmicb.2016.01542.
946 75. Cui F, Zhang N, Fan XL, Zhang W, Zhao CH, Yang LJ, et al. (2017). Utilization of a
947 Wheat660K SNP array-derived high-density genetic map for high-resolution mapping of a
948 major QTL for kernel number. Sci Rep. 2017;7: 3788. doi: 10.1038/s41598-017-04028-6.
949 76. Mansour E, Casas AM, Gracia AP, Molina-Cano JL, Moralejo M, Cattivelli L, et al.
950 Quantitative trait loci for agronomic traits in an elite barley population for Mediterranean
951 conditions. Mol Breed. 2014;33: 249–265.
952 77. Wang N, Chen B, Xu K, Gao G, Li F, Qiao J, et al. Association mapping of flowering time
953 QTLs and insight into their contributions to rapeseed growth habits. Front Plant Sci. 2016;7:
954 338. doi: 10.3389/fpls.2016.00338.
955 78. Hori K, Kobayashi T, Sato K, Takeda K. QTL analysis of Fusarium head blight resistance using
956 a high-density linkage map in barley. Theor Appl Genet. 2005;111: 1661–1672. doi:
957 10.1007/s00122-005-0102-4.
958 79. Horsley RD, Schmierer D, Maier C, Kudrna D, Urrea CA, Steffenson BJ, et al. Identification of
959 QTLs associated with Fusarium head blight resistance in barley accession CIho 4196. Crop Sci.
960 2006;46: 145–156. doi: 10.2135/cropsci2005.0247.
961 80. Massman J, Cooper B, Horsley R, Neate S, Dill-Macky R, Chao S, et al. Genome-wide
962 association mapping of Fusarium head blight resistance in contemporary barley breeding
963 germplasm. Mol Breed. 2011;27: 439–454. doi: 0.1007/s11032-010-9442-0.
964 81. Huang Y, Haas M, Heinen S, Steffenson BJ, Smith KP, Muehlbauer GJ. QTL mapping of
965 fusarium head blight and correlated agromorphological traits in an elite barley cultivar
966 Rasmusson. Front Plant Sci. 2018;9: 1260. doi: 10.3389/fpls.2018.01260.
967 82. Mamo BE, Steffenson BJ. Genome-wide association mapping of Fusarium head blight
968 resistance and agromorphological traits in barley landraces from Ethiopia and Eritrea. Crop Sci.
969 2015; 55: 1494–1512. doi: 10.2135/cropsci2014.06.0428.
970 83. Miedaner T, Heinrich N, Schneider B, Oettler G, Rohde S, Rabenstein F. Estimation of de-
971 oxynivalenol (DON) content by symptom rating and exoantigen content for resistance selection
972 in wheat and triticale. Euphytica. 2004;139: 123–132.
973 84. Šliková S, Šudyová V, Martinek P, Polišenská I, Gregová E, Mihálik D. Assessment of infection
974 in wheat by Fusarium protein equivalent levels. Eur J Plant Pathol. 2009;124: 163-–170.
975 85. Turner A, Beales J, Faure S, Dunford RP, Laurie DA. The pseudo-response regulator Ppd-H1
976 provides adaptation to photoperiod in barley. Science. 2005;310: 1031–1034.
977 86. Huang Y, Li L, Smith KP, Muehlbauer GJ. (2016). Differential transcriptomic responses to
978 Fusarium graminearum infection in two barley quantitative trait loci associated with Fusarium
979 head blight resistance. BMC Genomics. 2016;17: 387. doi: 10.1186/s12864-016-2716-0.
980 87. Nduulu L, Mesfin A, Muehlbauer G, Smith K. Analysis of the chromosome 2(2H) region of
981 barley associated with the correlated traits Fusarium head blight resistance and heading date.
982 Theor Appl Genet. 2007;115: 561–570. doi: 10.1007/s00122-007-0590-5.
983 88. He X, Osman M, Helm J, Capettini F, Singh PK.Evaluation of Canadian barley breeding lines
984 for Fusarium head blight resistance. Can J Plant Sci. 2015;95: 923–929.
985 89. Robertson A. The nature of quantitative genetic variation. In Heritage from Mendel (ed. Brink
986 A., editor. ), Madison, WI: The University of Wisconsin Press; 1967. pp. 265–280.
987 90. Kuczyńska A, Mikołajczak K, Ćwiek H. Pleiotropic effects of thesdw1 locus in barley
988 populations representing different rounds ofrecombination. Electron J Biotechnol. 2014;
989 17(5):217–223.
990 91. Wang J, Yang J, Jia Q, Zhu J, Shang Y, Hua W. et al. A new QTL for plant height in barley
991 (Hordeum vulgare L.) showing no negative effects on grain yield. PLoS ONE. 2014;9:e90144.
992 doi: 10.1371/journal.pone.0090144.

92. Kuczyńska A, Surma M, Adamski T, Mikołajczak K, Krystkowiak K, Ogrodowicz P. Effects of the semi-dwarfing sdw1/denso genein barley. J Appl Genet. 2013;54: 381–390.
93. Surma M, Kuczyńska A, Mikołajczak K, Ogrodowicz P, Adamski T, Ćwiek-Kupczyńska H, et al. Barley varieties in semi-controlled and natural conditions - response to water shortage and changing environmental parameters. J Agron Crop Sci. 2018;205(3).
94. Nakajima M, Shimada A, Takashi Y, Kim YC, Park SH, Ueguchi-Tanaka Me, et al.(2006). Identification and characterization of Arabidopsis gibberellin receptors. The Plant J. 2006;46: 880–889.
95. Mikołajczak K, Kuczynska A, Krajewski P, Sawikowska A, Surma M, Ogrodowicz P, et al. Quantitative trait loci for plant height in Maresi × CamB barley population and their associations with yield-related traits under different water regimes. J Appl Genet. 2017;58: 23–35.
96. Paul PA, El-Allaf SM, Lipps PE, Madden LV. Rain splash dispersal of Gibberella zeae within wheat canopies in Ohio. Phytopathology. 2004;94: 1342–1349. doi: 10.1094/PHYTO.2004.94.12.1342.
97. Nadolska-Orczyk A, Rajchel IK, Orczyk W, Gasparis S. Major genes determining yield-related traits in wheat and barley. Theor Appl Genet. 2017;130(6): 1081–98. WOS:000401980500001. pmid:28314933.
98. Choo TM, Vigier B, Shen QQ, Martin RA, Ho KM, Savard M. Barley traits associated with resistance to fusarium head blight and deoxynivalenol accumulation. Phytopathology. 2004;94: 1145–1150.
99. Langevin F, Eudes F, Comeau A. 2004. Effect of trichothecenes produced by Fusarium graminearum during Fusarium head blight development in six cereal species. Eur J Plant Pathol. 2004;110: 735–746.
100. Li XX, Zhu B, Gao XW, Liang P. Over-expression of UDP-glycosyltransferase gene UGT2B17 is involved in chlorantraniliprole resistance in Plutella xylostella (L.) Pest Manag Sci. 2017;73: 1402–1409.
101. Xing Z, Geng W, Li C, Sun Y, Wang Y. (2017). Comparative genomics of Lactobacillus kefiranofaciens ZW3 and related members of Lactobacillus. spp reveal adaptations to dairy and gut environments. Sci Rep. 2017;7: 12827. doi: 10.1038/s41598-017-12916-0.
102. Gachon CM, Langlois-Meurinne M, Saindrenan P. Plant secondary metabolism glycosyltransferases: the emerging functional analysis. Trends Plant Sci. 2005;10(11): 542–549.
103. Caputi L, Malnoy M, Goremykin V, Nikiforova S, Martens S. A genome-wide phylogenetic reconstruction of family 1 UDP-glycosyltransferases revealed the expansion of the family during the adaptation of plants to life on land. Plant J. 2012;69: 1030–1042.
104. Poppenberger B, Berthiller F, Lucyshyn D, Sieberer T, Schuhmacher R, Krska R, et al. Detoxification of the Fusarium mycotoxin deoxynivalenol by a UDP-glucosyltransferase from Arabidopsis thaliana. J Biol Chem. 2003;278: 47905–47914.
105. Van Loon LC, Van Strien EA. The families of pathogenesis-related proteins, theiractivities, and comparative analysis of PR-1 type proteins. Physiol Mol Plant Pathol. 1999;55: 85–97.
106. Pritsch C, Muehlbauer GJ, Bushnell WR, Somers DA, Vance CP. Fungal development and induction of defense response genes during early infection of wheat spikes by Fusarium graminearum. Mol Plant Microbe Interact. 2000;13: 159–169.
107. Balasubramanian V, Vashisht D, Cletus J, Sakthivel N. Plant β-1,3-glucanases: Their biological functions and transgenic expression against phytopathogenic fungi. Biotechnol Lett. 2012;34(11):1983–90. doi: 10.1007/s10529-012-1012-6.
108. Robert-Seilaniantz A, Navarro L, Bari R, Jones JD. Pathological hormone imbalances Curr. Opin. Plant Biol. 2007;10: 372–379.
109. Petti C, Reiber K, Ali SS, Berney M, Doohan FM. Auxin as a player in the biocontrol of Fusarium head blight disease of barley and its potential as a disease control agent. BMC Plant Biol. 2012;12: 224. doi: 10.1186/1471-2229-12-224.

110. Denancé N, Sánchez-Vallet A, Goffner D, Molina A. 2013.Disease resistance or growth: the role of plant hormones inbalancing immune responses and fitness costs. Front Plant Sci. 2013;4: 155.
111. Wang K, Guo Q, Froehlich JE, Hersh HL, Zienkiewicz A, Howe GA, Benning C. Two Abscisic Acid-Responsive Plastid Lipase Genes Involved in Jasmonic Acid Biosynthesis in Arabidopsis thaliana. The Plant Cell. 2018;30(5): 1006-1022. doi: 10.1105/tpc.18.00250.
112. Gottwald S, Samans B, L ̈uck S, Friedt W. Jasmonate and ethylene dependent defence gene expression and suppression of fungal virulence factors: Two essential mechanisms of Fusarium head blight resistancein wheat? BMC Genomics. 2012;13: 369.
113. Ford B, Deng W, Clausen J, Oliver S, Boden S, Hemming M, et al. Barley (Hordeum vulgare) circadian clock genes can respond rapidly to temperature in an EARLY FLOWERING 3-dependent manner. J Exp Bot. 2016; 67(18):5517–5528. doi: 10.1093/jxb/erw317.
114. Fercha A, Capriotti AL, Caruso G, Cavaliere C, Gherroucha H, Samperi R, et al. Gel-free proteomics reveal potential biomarkers of priming-induced salt tolerance in durum wheat. J Proteomics. 2013;91: 486–499. 10.1016/j.jprot.2013.08.010.
115. Ghabooli M, Khatabi B, Ahmadi FS, Sepehri M, Mizraei M, Amirkhani A, et al. Proteomics study reveals the molecular mechanisms underlying water stress tolerance induced by Piriformospora indica in barley. J Proteomics. 2013;94:289–301. doi: 10.1016/j.jprot.2013.09.017
116. Stone SL, Callis J. Ubiquitin ligases mediate growth and development by promoting protein death. Curr Opin Plant Biol. 2007;10: 624–632. doi: 10.1016/j.pbi.2007.07.010.

Figure1

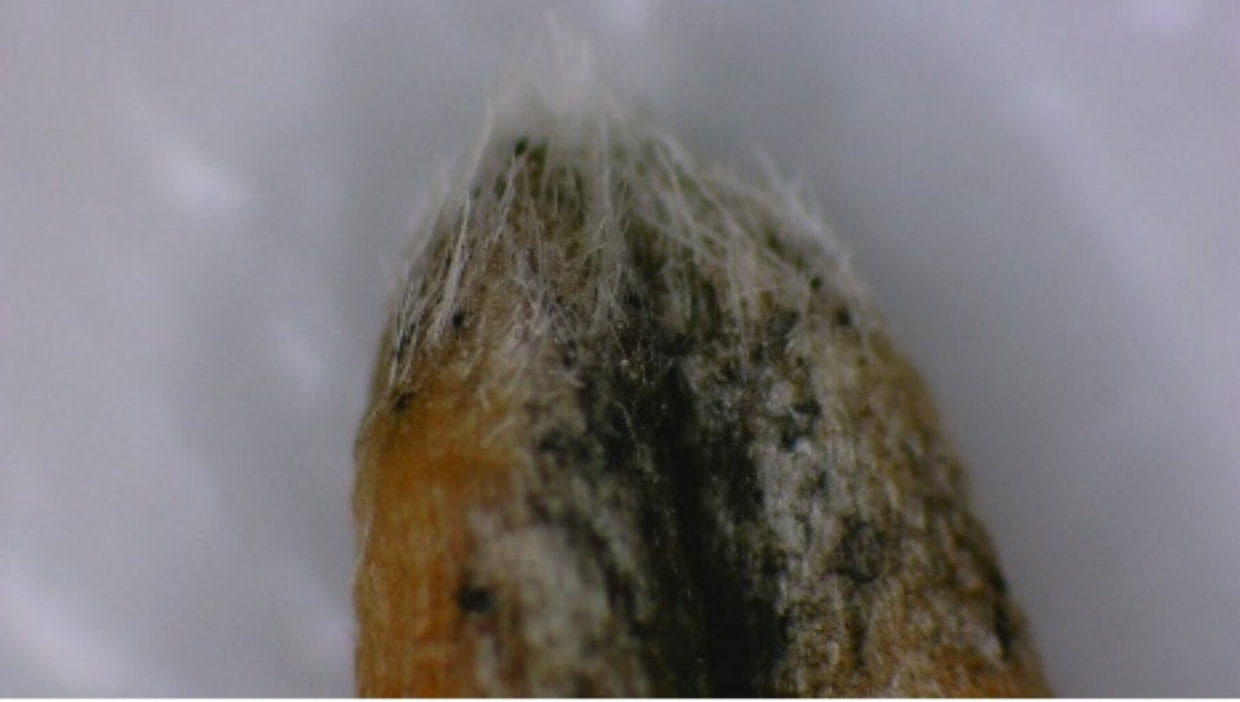

Figure2

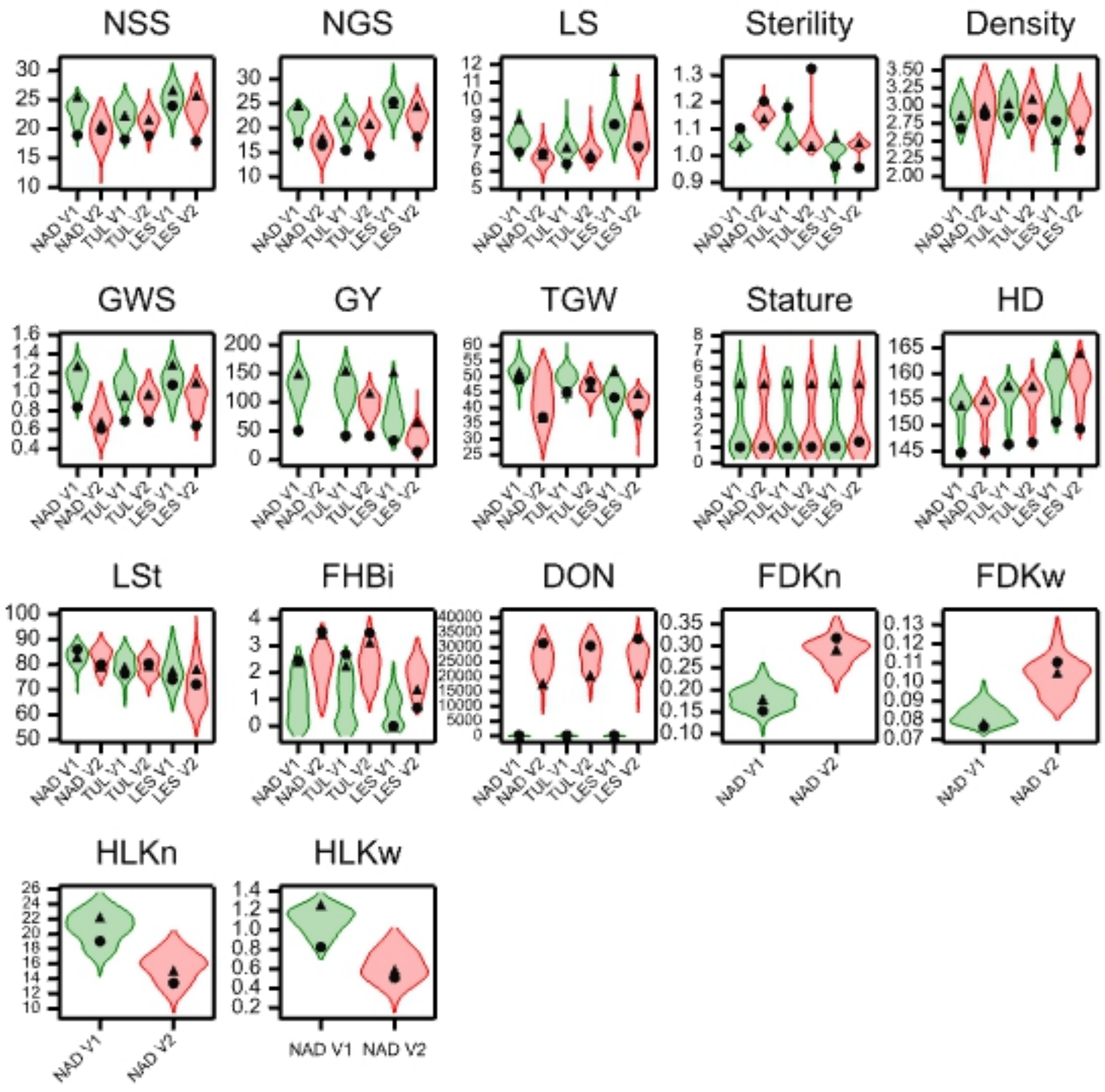
NSS
NGS
LS
Sterility
Density
GWS
GY
TGW
Stature
HD
LSt
FHBi
DON
FDKn
FDKw
HLKn
HLKw
NAD V1
NAD V2
TUL V1
TUL V2
LES V1
LES V2

Figure3

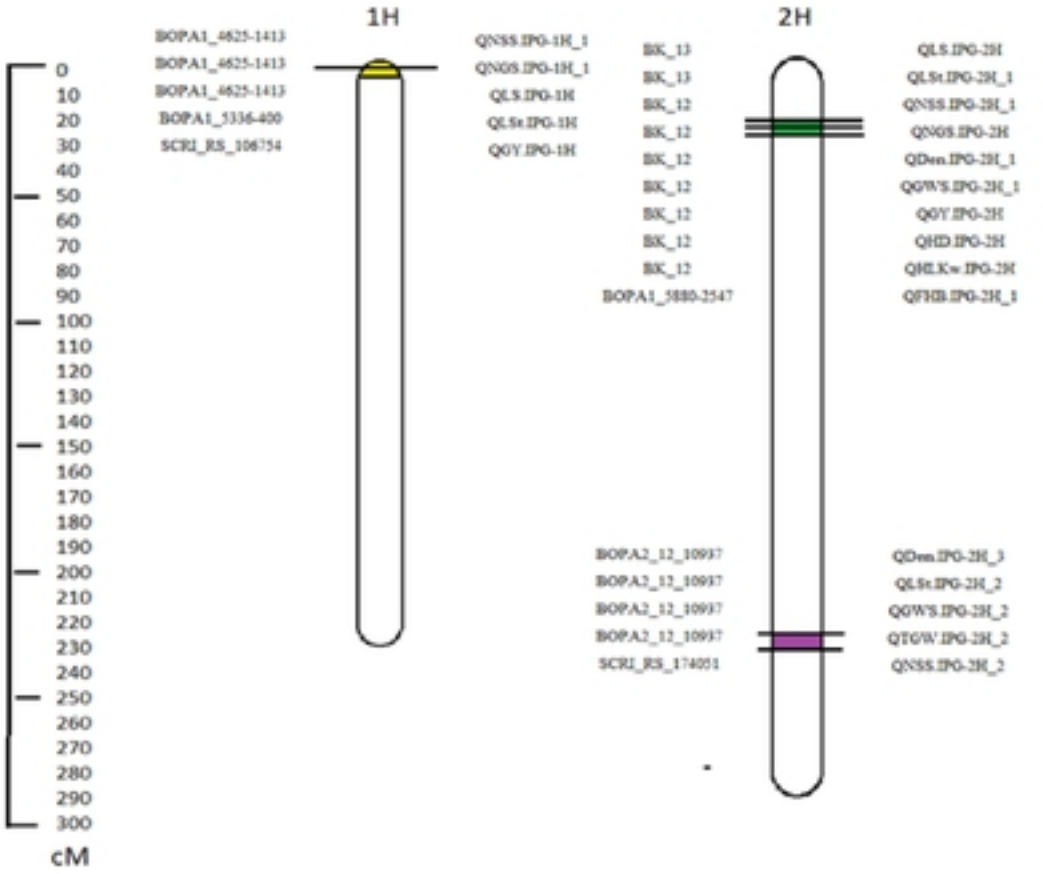
1H
2H
0
10
20
30
40
50
60
70
80
90
100
110
120
130
140
150
160
170
180
190
200
210
220
230
240
250
260
270
280
290
300
cM
BOPA1_4625-1413
BOPA1_4625-1413
BOPA1_4625-1413
BOPA1_5336-400
SCRI_RS_106754
QNSS.IPG-1H_1
QNGS.IPG-1H_1
QLS.IPG-1H
QLSt.IPG-1H
QGY.IPG-1H
BK_13
BK_13
BK_12
BK_12
BK_12
BK_12
BK_12
BK_12
BK_12
BOPA1_5880-2547
QLS.IPG-2H
QLSt.IPG-2H_1
QNSS.IPG-2H_1
QNGS.IPG-2H
QDen.IPG-2H_1
QGWS.IPG-2H_1
QGY.IPG-2H
QHD.IPG-2H
QHLKw.IPG-2H
QFHB.IPG-2H_1
BOPA2_12_10937
BOPA2_12_10937
BOPA2_12_10937
BOPA2_12_10937
SCRI_RS_174051
QDen.IPG-2H_3
QLSt.IPG-2H_2
QGWS.IPG-2H_2
QTGW.IPG-2H_2
QNSS.IPG-2H_2

Figure4